

**UNCLASSIFIED**

---

---

**AD 402 382**

*Reproduced  
by the*

**DEFENSE DOCUMENTATION CENTER**

FOR

**SCIENTIFIC AND TECHNICAL INFORMATION**

CAMERON STATION, ALEXANDRIA, VIRGINIA



---

---

**UNCLASSIFIED**

NOTICE: When government or other drawings, specifications or other data are used for any purpose other than in connection with a definitely related government procurement operation, the U. S. Government thereby incurs no responsibility, nor any obligation whatsoever; and the fact that the Government may have formulated, furnished, or in any way supplied the said drawings, specifications, or other data is not to be regarded by implication or otherwise as in any manner licensing the holder or any other person or corporation, or conveying any rights or permission to manufacture, use or sell any patented invention that may in any way be related thereto.

63-3-2

CATALOGED BY ASTIA 4 023 82  
AS FILED

AMRL-TDR-63-11

# 402 382

## DISPLAY SYSTEMS FOR SUB- AND ZERO-GRAVITY FLIGHT

TECHNICAL DOCUMENTARY REPORT NO. AMRL-TDR-63-11

January 1963

Behavioral Sciences Laboratory  
6570th Aerospace Medical Research Laboratories  
Aerospace Medical Division  
Air Force Systems Command  
Wright-Patterson Air Force Base, Ohio

Contract Monitor: Melvin S. Gardner, Captain, USAF  
Project No. 7184, Task No. 718405

[Prepared Under Contract No. AF 33(657)-7199  
by  
Robert Weiss  
Lear Siegler, Inc.  
Grand Rapids, Michigan]

ASTIA  
APR 11 1963  
15

## NOTICES

When US Government drawings, specifications, or other data are used for any purpose other than a definitely related government procurement operation, the government thereby incurs no responsibility nor any obligation whatsoever; and the fact that the government may have formulated, furnished, or in any way supplied the said drawings, specifications, or other data is not to be regarded by implication or otherwise, as in any manner licensing the holder or any other person or corporation, or conveying any rights or permission to manufacture, use, or sell any patented invention that may in any way be related thereto.

Qualified requesters may obtain copies from ASTIA. Orders will be expedited if placed through the librarian or other person designated to request documents from ASTIA.

Do not return this copy. Retain or destroy.

Stock quantities available at Office of Technical Services, Department of Commerce, \$1.75.

### Change of Address

Organizations receiving reports via the 6570th Aerospace Medical Research Laboratories automatic mailing lists should submit the addressograph plate stamp on the report envelope or refer to the code number when corresponding about change of address.

<p>Aerospace Medical Division, 6570th Aerospace Medical Research Laboratories, Wright-Patterson AFB, Ohio Rpt. No. AMRL-TDR-63-11. DISPLAY SYSTEMS FOR SUB- AND ZERO- GRAVITY FLIGHT Final Report Jan 63, x + 54 pp. incl. illus., tables, 26 refs. Unclassified report</p> <p>A study was performed of the controls and pilot displays used to fly a C-131B and KC-135 aircraft in a Keplerian trajectory to create zero-gravity conditions. Evaluation criteria for this maneuver were proposed and applied to two basic instrumentation systems which were developed. An analog simulation was formulated and these results will be used to further improve the systems.</p> <p style="text-align: right;">( over )</p>	<p>Aerospace Medical Division, 6570th Aerospace Medical Research Laboratories, Wright-Patterson AFB, Ohio Rpt. No. AMRL-TDR-63-11. DISPLAY SYSTEMS FOR SUB- AND ZERO- GRAVITY FLIGHT Final Report Jan 63, x + 54 pp. incl. illus., tables, 26 refs. Unclassified report</p> <p>A study was performed of the controls and pilot displays used to fly a C-131B and KC-135 aircraft in a Keplerian trajectory to create zero-gravity conditions. Evaluation criteria for this maneuver were proposed and applied to two basic instrumentation systems which were developed. An analog simulation was formulated and these results will be used to further improve the systems.</p> <p style="text-align: right;">( over )</p>	<p>UNCLASSIFIED</p> <p>1. Keplerian Trajectory 2. Weightlessness 3. Control and Pilot Displays 4. Analog Simulation 5. Instrument Panels I. AFSC Project 7184, Task 718405 II. Behavioral Sciences Laboratory Contract AF 33(657)- 7199 IV. Lear Siegler, Inc. Grand Rapids, Mich. V. R. Weiss</p> <p>UNCLASSIFIED</p>	<p>UNCLASSIFIED</p> <p>1. Keplerian Trajectory 2. Weightlessness 3. Control and Pilot Displays 4. Analog Simulation 5. Instrument Panels I. AFSC Project 7184, Task 718405 II. Behavioral Sciences Laboratory Contract AF 33(657)- 7199 IV. Lear Siegler, Inc. Grand Rapids, Mich. V. R. Weiss</p> <p>UNCLASSIFIED</p>
<p>UNCLASSIFIED</p> <p>VI. In ASTIA collection VII. Aval fr OTS: \$1.75 at zero-gravity plus or minus 0.005g.</p> <p>UNCLASSIFIED</p>	<p>UNCLASSIFIED</p> <p>VI. In ASTIA collection VII. Aval fr OTS: \$1.75 at zero-gravity plus or minus 0.005g.</p> <p>UNCLASSIFIED</p>	<p>UNCLASSIFIED</p> <p>VI. In ASTIA collection VII. Aval fr OTS: \$1.75</p> <p>UNCLASSIFIED</p>	<p>UNCLASSIFIED</p> <p>VI. In ASTIA collection VII. Aval fr OTS: \$1.75</p> <p>UNCLASSIFIED</p>

## FOREWORD

This study was initiated by the Behavioral Sciences Laboratory, 6570th Aerospace Medical Research Laboratories, Aerospace Medical Division, Wright-Patterson Air Force Base, Ohio, and the Control Synthesis Branch, Flight Control Laboratory, Directorate of Aeromechanics, Aeronautical Systems Division, Wright-Patterson Air Force Base, Ohio. The work was performed by Lear Siegler, Inc., Grand Rapids, Michigan, under Contract No. AF 33(657)-7199. Captains C. E. Waggoner and M. S. Gardner of the Crew Stations Section were the contract monitors for the Behavioral Sciences Laboratory. The work was performed in support of Project No. 7184, "Human Performance in Advanced Systems," and Task No. 718405, "Design Criteria for Crew Stations in Advanced Systems." The work sponsored by this contract was started in August 1961 and completed in March 1962.

Acknowledgement is made to the following individuals who aided in this study: Capt. J. C. Simons of the Crew Stations Section for his help in implementing many of the phases of the research, Sgts. Sears and Espensen for their invaluable assistance during the flight tests and instrumentation in the C-131B, Maj. E. M. Sommerich of the Flight Research Section of the Control Synthesis Branch for instrumentation and equipment support, and to the personnel of Lear Siegler, Inc. for their technical aid.

#### ABSTRACT

A study was performed of the controls and pilot displays used to fly a C-131B and KC-135 aircraft in a Keplerian trajectory to create zero-gravity conditions. Evaluation criteria for this maneuver were proposed and applied to two basic instrumentation systems which were developed. An analog simulation was formulated and these results will be used to further improve the systems. Recommendations are made for improved instrumentation which should enable consistent flights of 10 seconds at zero-gravity plus or minus 0.005g.

#### PUBLICATION REVIEW

This technical documentary report has been reviewed and is approved.

*Walter F. Grether*

WALTER F. GREYER  
Technical Director  
Behavioral Sciences Laboratory

## TABLE OF CONTENTS

	Page
INTRODUCTION	1
I HISTORY	2
II EQUIPMENT DESCRIPTION	5
A. 3 Axis Accelerometer Read-Out (C-131B)	5
B. KC-135 Accelerometer Reference	8
C. Closed Circuit Television	9
D. Revision B, ADI Modification (C-131B)	10
III TESTS PERFORMED	20
A. Level of Accuracy and Measures of Goodness	20
B. Display Gain <u>Vs.</u> Accuracy	21
C. Three Axis Accelerometer <u>Vs.</u> Revision B ADI Modification System Accuracies	25
D. KC-135 Instrumentation Accuracy	25
IV FUTURE WORK INDICATED	27
A. Revision D System	27
B. Analog Simulation	29
C. Varying Display Gain and Compensation	30
D. Autopilot Controlled Zero-G	30
APPENDICES	
Bibliography	32
A. Equipment Leading Particulars	35
B. Tabular Data	39
C. Development of Simulation Equations	47

## LIST OF ILLUSTRATIONS

FIGURE NO.	TITLE	PAGE
1	Zero-Gravity Flight Path	2
2	C-131B Cockpit	3
3	Free Floating Cork	4
4	Three Axis Accelerometer Package-Control Box	5
5	Remote Acceleration Readout	5
6	Three Axis Accelerometer Read-Out Schematic	7
7	Wiring Diagram-Accelerometer Installation, KC-135	8
8	Closed Circuit T. V. Installation, C-131B	9
9	Attitude Director Indicator	10
10	Revision B, ADI Modification Schematic	11
11	Pilot's Panel - ADI Modification	12
12	ADI Modification Instrument Installation	13
13	Donner Accelerometer Installation	13
14	Control Rack R-7, Revision B, ADI Modification	14
15	Diode Limiter Transfer Characteristic	15
16	G-Level Selector and Isolation Amplifier - Installation	16
17	G-Level Selector and Isolation Amplifier - Schematic	16
18	G-Level Selector-Vernier Setting Vs. G-Level	17
19	G-Level Selector - Transfer Characteristic	17
20	Accelerometer Signal Simulator-Schematic	18
21	Accelerometer Simulator in Use	18
22	Typical Parabola-Significant Points	20
23	Diagram Illustrating "Time-Within-Tolerance"	21

LIST OF ILLUSTRATIONS (Cont'd)

FIGURE NO.	TITLE	PAGE
24	Time Within Tolerance <u>VS.</u> Display Gain	22
25	Distance From Parabola Apex <u>VS.</u> Display Gain	23
26	Maximum Error <u>VS.</u> Display Gain	23
27	Initial Overshoot <u>VS.</u> Display Gain	23
28	System Step Responses	24
29	Trace Showing Oscillatory Characteristic	24
30	Histogram of System Characteristic Frequencies	24
31	Proposed Revision D System Block Diagram	28
32	Analog Simulation-Block Diagram	29
33	Definition of Axes and Angles	48
34	Pilot Model	53
35	Arbitrary Function Generator (G-Programmer)	53

LIST OF TABLES

TABLE NO.	TITLE	PAGE
1	Summary of the Data From Four C-131B Flights	40
2	Unprocessed Data-- C-131B Flight of 16 October 1961	40
3	Unprocessed Data-- C-131B Flight of 18 October 1961	41
4	Unprocessed Data-- C-131B Flight of 27 October 1961	42
5	Unprocessed Data-- C-131B Flight of 30 October 1961	42
6	Distance From Parabola Apex of $T_{O3}$	43
7	Unprocessed Data-- C-131B Flight of 3 January 1962	44
8	Summary of Data From Eleven KC-135 Flights	45
9	Typical KC-135 Stopwatch Float Times	46

LIST OF SYMBOLS

$X_i$	Force along the aircraft longitudinal axis due to parameter "i"
$Z_i$	Force along the aircraft normal axis due to parameter "i"
$M_i$	Moment about the aircraft lateral axis due to parameter "i"
$Q$	Rotation of body axis system about lateral axis
$U$	Component of total aircraft velocity in X direction
$W$	Component of total aircraft velocity in Z direction
$V_p$	Total aircraft inertial velocity
$I_{yy}$	Moment of inertia of aircraft about Y axis
$m$	Mass of aircraft
$l$	Distance between C.G. and normal accelerometer
$g$	Acceleration of gravity
$\theta$	Euler pitch angle
$\rho$	Air density
$S$	Total wing area
$\alpha$	Angle of attack
$\delta_e$	Elevator deflection
$\bar{c}$	Mean aerodynamic chord
$S_x$	Horizontal position wrt earth (E-W)
$C_{D\delta_e}$	Change of coefficient of drag due to elevator deflection
$S_z$	Altitude above sea level
$C_{D_0}$	Equilibrium drag constant
$C_L$	Coefficient of lift
$C_{D\alpha}$	Change of coefficient of drag due to angle of attack
$C_D$	Drag Coefficient

LIST OF SYMBOLS (cont'd)

$C_{L\alpha}$	Coefficient of lift due to angle of attack
$C_{L\dot{\alpha}}$	Coefficient of lift due to change in angle of attack
$C_{LQ}$	Coefficient of lift due to pitch body rate
$C_{L\delta_e}$	Coefficient of lift due to elevator deflection
$C_{m\alpha}$	Moment coefficient due to angle of attack
$C_{mQ}$	Moment coefficient due to pitch body rate
$C_{m\dot{\alpha}}$	Moment coefficient due to change in angle of attack
$C_{m\delta_e}$	Moment coefficient due to elevator deflection
T	Thrust force
$K_p$	Pilot gain
$T$	Pilot reaction time constant
$T_L$	Pilot lead term time constant
$T_I$	Pilot lag term time constant
$T_N$	Pilot neuromuscular lag time constant
s	LaPlace Operator
$K_{\delta_e}$	Quickening gain
$K_{rpm}$	Throttle gain
$K_{cp}$	Co-pilot gain
$K_{td}$	Throttle Display gain

Subscripts

T	Thrust
Q	Body rotation about Y axis
g	Gravity
s	Stability axis

LIST OF SYMBOLS (cont'd)

$u$	Forward velocity
$o$	Steady state
$\alpha$	Angle of attack
$\delta e$	Elevator deflection
$\int \text{rpm}$	Change of rpm due to throttle deflection

Dotted quantities refer to rate of change of quantity

## INTRODUCTION

The effect of a prolonged zero-gravity field on many physiological, psychological and physical processes remain unknown. Economic factors preclude the use of actual orbital missions as a means of investigating all of the possible effects, and ground-based methods of simulating zero-gravity either produce too-short periods (elevators) or imperfect simulated zero-gravity (submersion tanks). A method was therefore developed for producing a true zero-gravity field by means of flying specific maneuvers in aircraft. The range of zero-g time using this method is from seconds to minutes. Even this short time span has enabled many experimenters to conduct important research in the functioning of humans and preliminary evaluations of machines functioning in a zero-gravity field (Ref.2).

This report describes the research performed through March 1962 in producing the sub- and zero-gravity state by means of flight in the C-131B and KC-135A aircraft at Wright-Patterson Air Force Base. The report describes the flight path and condition recording instrumentation. The emphasis is placed on improving display methods in piloted flight with the ultimate aim of providing accurate and reproducible automatic flight paths according to the needs of the zero-gravity researchers.

## SECTION I - HISTORY

A history and description of the various methods of producing and simulating zero-gravity may be found in Reference 1. The zero-gravity state can be produced by flying aircraft on a ballistic trajectory. The specific trajectory to fulfill the necessary conditions for this state is an approximation of a parabolic arc with a vertical axis. Actual maneuver parameters for any given aircraft are determined by the specific aerodynamic characteristics of the aircraft. Important parameters are maximum allowable airspeed, structural loading and stall speed.

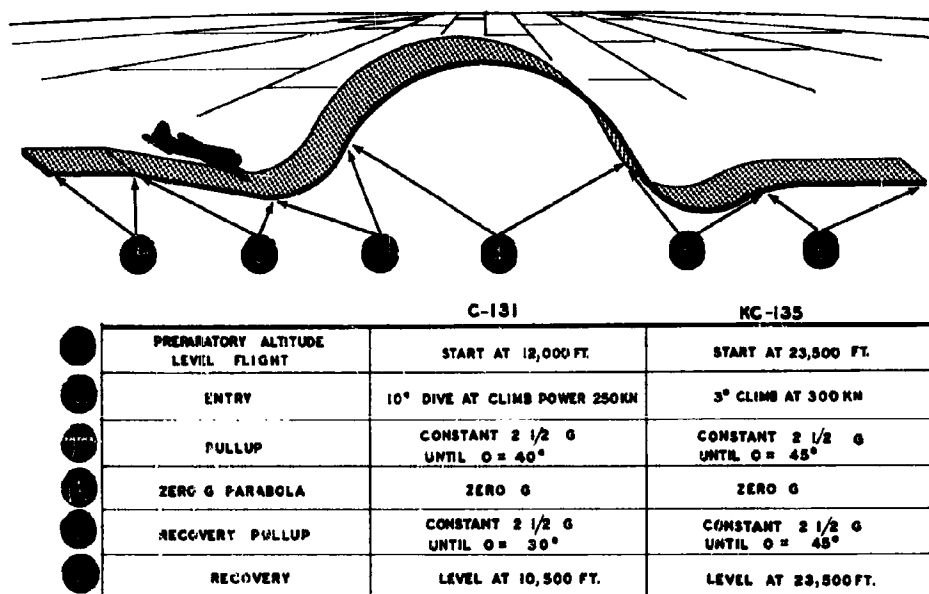


Figure 1. Zero-Gravity Flight Path

A typical parabola (Figure 1) includes the following phases: Phase 1, the preparatory phase is flown at cruise speed and constant altitude. The typical starting altitude for the C-131 is 12,000 feet and for the KC-135 is approximately 24,000 feet. At Phase 2, the airspeed is increased to a safe maximum by applying military rated thrust power, and in the case of the C-131, entering the aircraft into a 10° dive. When the speeds of 250 and 374 knots indicated air speed for the C-131 and KC-135, respectively, are reached, the aircraft enters into Phase 3, the entry pullup. The pilot executes this phase at a constant 2-1/2 g normal acceleration, which he holds until a precalculated pitch attitude is reached. This pitch angle is one of the important determining factors of parabola duration, and is about 35 degrees climb for the C-131 and 45 degrees climb for the KC-135. These figures were determined initially by

analog computer studies of the two aircraft, and were optimized in flight testing. When the optimum pitch attitude is reached, the pilot enters into the zero-gravity phase, Phase 4, which he holds until the aircraft achieves its precalculated nose-down attitude of 30° for the C-131 or 45° for the KC-135. At this point the recovery pullup, Phase 5, is initiated at 2-1/2 g and the aircraft is either leveled out, or enters into another parabola. Early methods of zero-g flight consisted of flying the aircraft around floating objects. The first floating object to be used as a flight reference in the C-131 aircraft was the pilot's wallet, which was placed on the top of the instrument panel. The aircraft was flown about the floating wallet to produce nominal zero-gravity.

There are two types of zero-gravity flight which will be referred to in this report. The first concerns flying the aircraft in zero-gravity conditions for strapdown experiments, and the second type is concerned with free-floating experiments. For the latter maneuver, the aircraft flies a nominal zero-gravity trajectory about the experimental capsule. The capsule is under near-perfect zero-gravity, although the airframe is not necessarily gravity free.

Following the "wallet instrumentation," experiments were performed with a golf ball suspended by two rubber bands. At zero-gravity the golf ball, having no apparent weight, would assume a horizontal position (Number 2 in Figure 2) being held only by the tension of the two rubber bands on its opposite sides. The golf ball supplemented a G-meter (Number 1 in Figure 2).

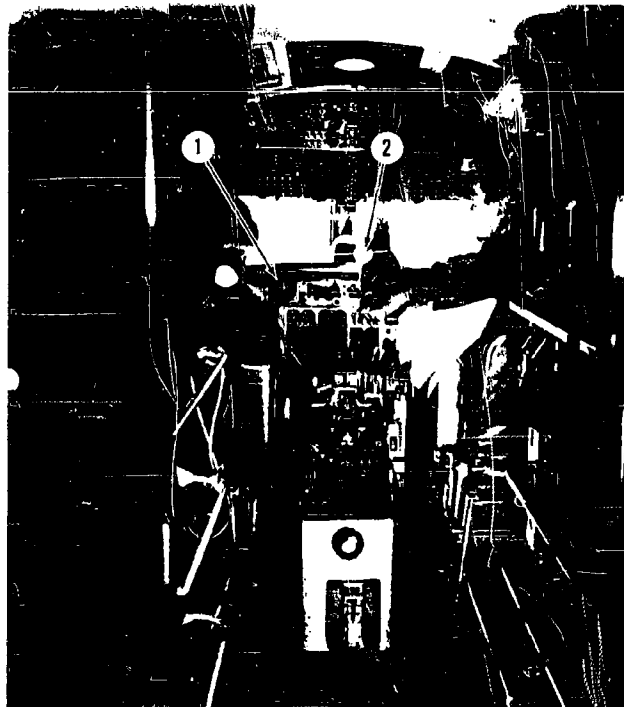


Figure 2. C-131B Cockpit

Another type of golf ball instrumentation is presently being used at Brooks AFB in the zero-gravity flights of the F-100F aircraft. The golf ball in this case is suspended by a six to eight inch string below the over-head panel in plain view of the pilot. The pilot flies the airplane about the floating golf ball.

The next type of instrumentation used on the C-131 was the free-floating cork. This instrument consisted of a fluid-filled six-inch plastic sphere mounted above the glare shield. Floating in the fluid was a round cork attached to a string and a crank at the bottom of the instrument (Figure 3). The string and crank were used to reset the cork to the middle of the sphere at the start of the zero-g parabola. The pilot "flew the cork," attempting to maintain the cork in the middle of the sphere. At this point in the history of the C-131B zero-g instrumentation, the emphasis was switched to accelerometer-based references. A sensitive linear accelerometer was used to provide a normal acceleration display on a pilot's indicator. Heading hold and wings level established (hopefully) zero lateral acceleration, and co-pilot control of the throttles was used to control longitudinal acceleration. This arrangement was very similar to that described by Schock (Reference 8).

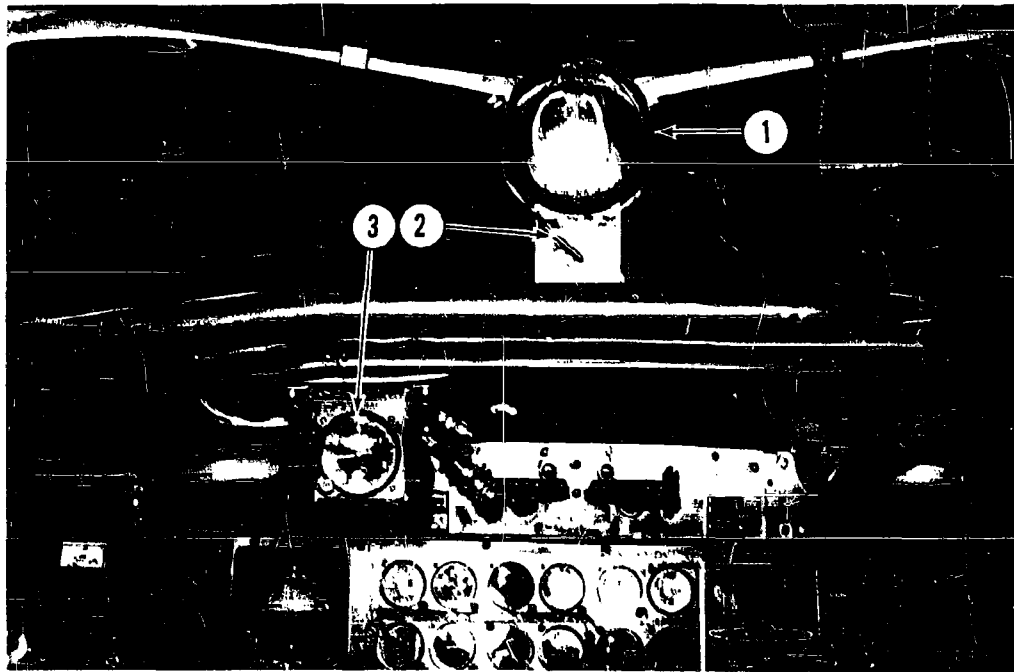


Figure 3. Free Floating Cork

## SECTION II - EQUIPMENT DESCRIPTION

### A. THREE-AXIS ACCELEROMETER READOUT (C-131B)

This instrument system provides an oscillograph record of the acceleration in the three aircraft body axes, gives an instantaneous meter readout for the operator amidships, provides a longitudinal remote readout for the co-pilot for throttle control and provides a back-up primary normal-g reference for the pilot in case of failure or non-function of the other zero-g instrumentation.

Physically, the system may be broken down into three parts. Primary sensors are three strain-gauge accelerometers with  $\pm 5g$  range, mounted orthogonally and fastened to Equipment Rack L-8 in line with the aircraft's primary axes. Calibration, balance, amplifier and meter circuitry are contained in a control box, shock mounted on Rack L-7 (Figure 4). The pilot's or co-pilot's remote readout, (Figure 5) is mounted beneath the instrument panel glare shield.

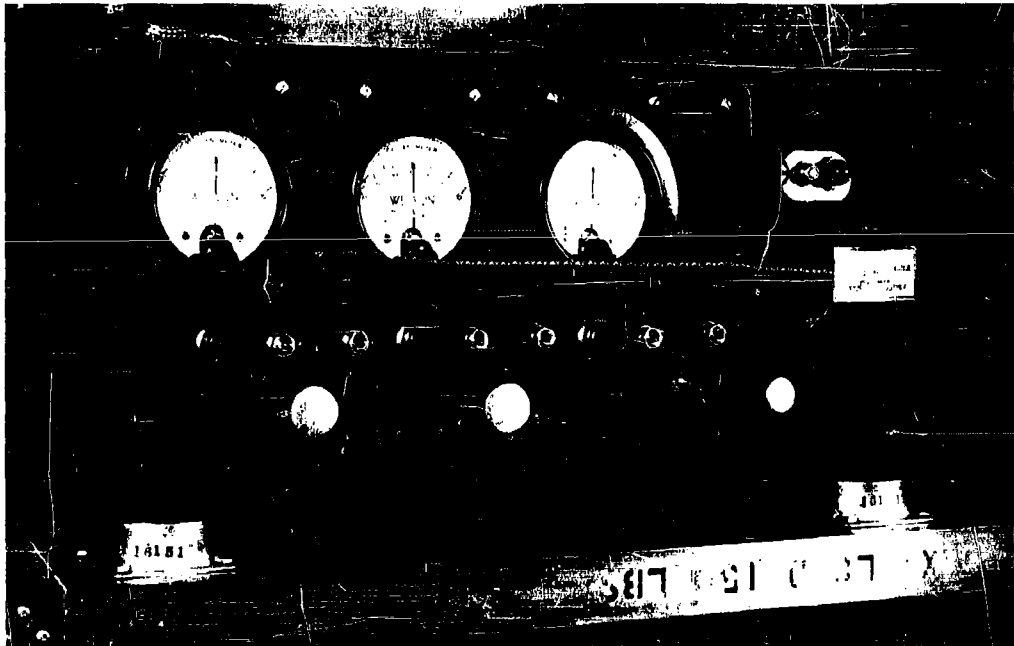


Figure 4.  
Three Axis Accelerometer Package -  
Control Box

The sensors are B&F Instruments, Inc. linear strain-gauge accelerometers, Model LF5-20-350. The strain-gauge balance and calibration circuitry (Figure 6) are found in the three axis control box. The accelerometer signals are amplified by Doelcam Model ZHMA-2 D.C. amplifiers. The amplified acceleration signals are presented on sensitive meters on the face of the control box with a gain-changing network incorporated to switch meter sensitivities at  $\pm 0.3$  g. The double range gives meter sensitivities of  $\pm 3g$ /full scale and  $\pm 0.3g$ /full scale. A signal light for each meter tells which scale the meter is indicating. In addition to the three meter read-outs, the amplifier outputs are routed through galvanometer compensation and gain networks to a recording oscillograph for a permanent record of the 3 axis aircraft accelerations during the parabolic maneuver. The Remote Readout (Figure 5) consists of identical relay and meter circuits with provision to monitor any of the three channels. In the usual configuration it is used as a longitudinal display for co-pilot throttle control. On occasion, it is used by the pilot as a primary normal-g reference. There is provision in the C-131B aircraft to mount the remote readout either in front of the pilot or the co-pilot.

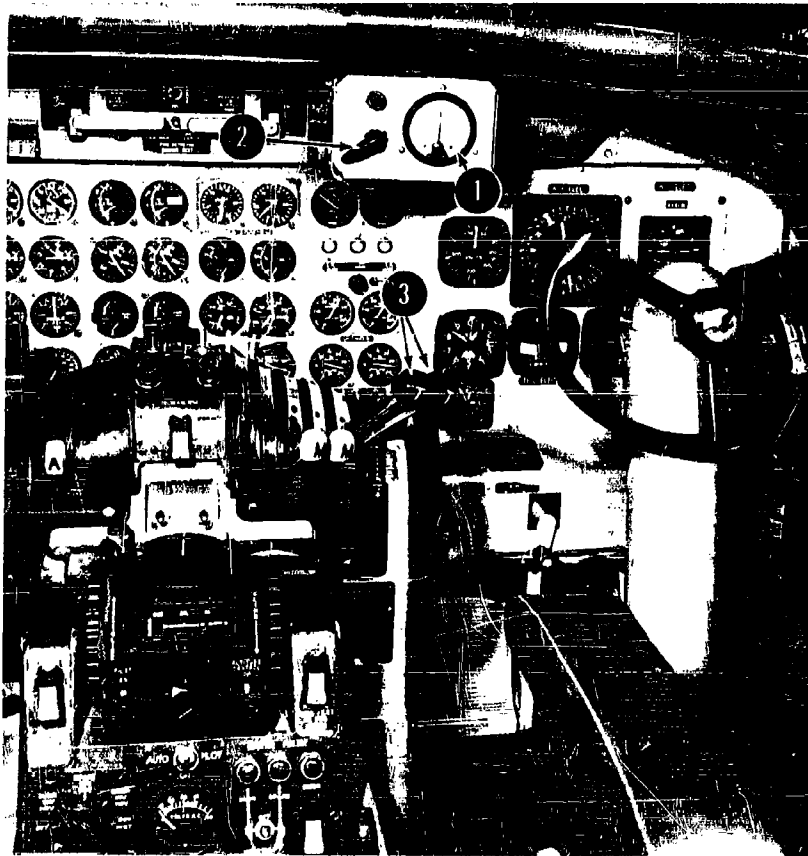
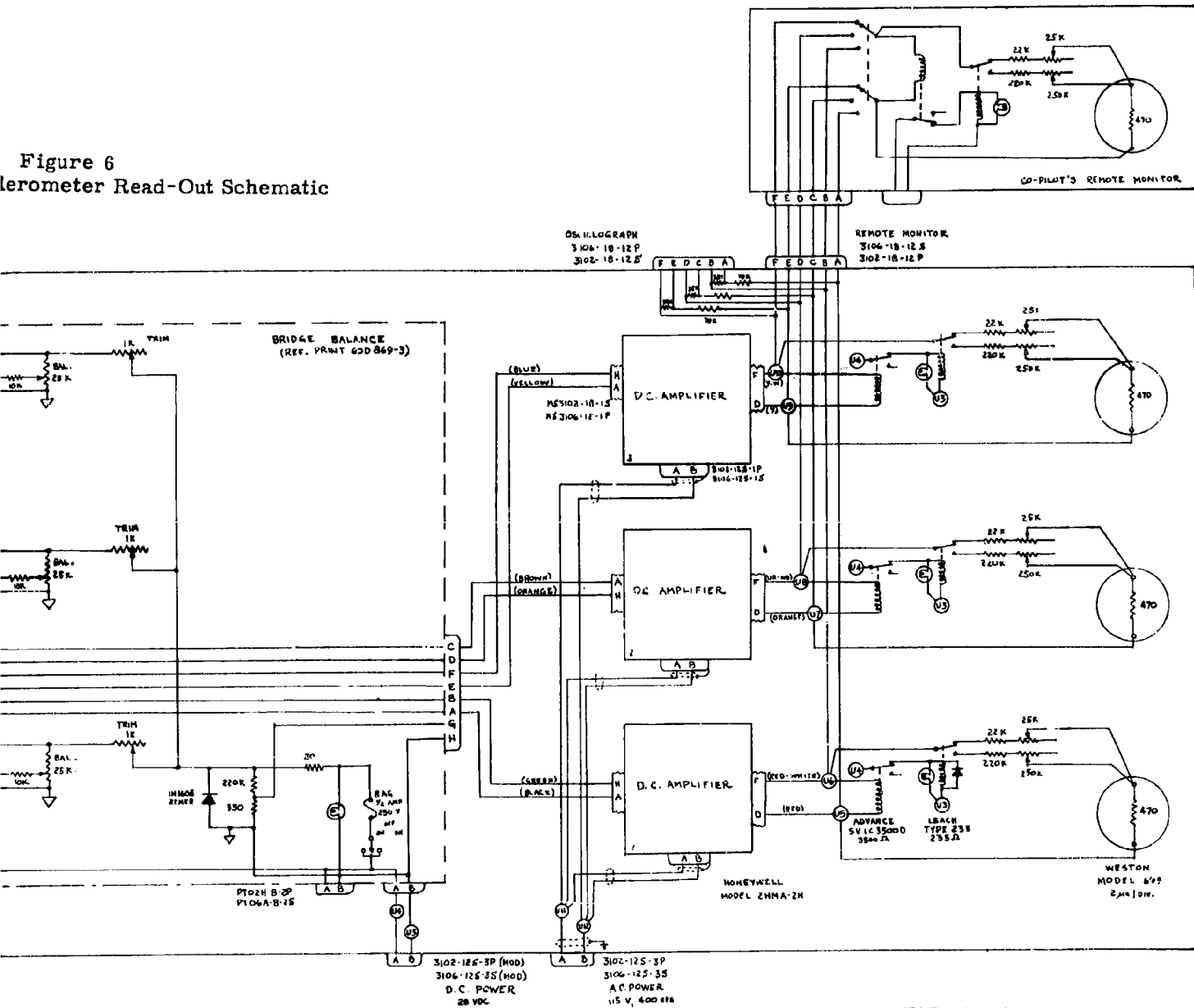


Figure 5.  
Remote Acceleration Readout



Figure 6  
Thermometer Read-Out Schematic



2

B. KC-135 ACCELEROMETER REFERENCE

The instrumentation presently installed in the zero-g KC-135 was designed and installed by Boeing Airplane Company as part of an overall conversion of aircraft Serial Number 55-3129 for zero-gravity service. A wiring diagram of the installation appears as Figure 7 of this report, with accelerometer particulars in Appendix B. The installation is fully described in Reference 3.

The basic three-axis acceleration reference consists of three orthogonally mounted Donner Model 4310 fluid-damped force-balance linear accelerometers mounted on the floor at Station 850 and aligned with the aircraft's primary axes. Signals from the normal and longitudinal accelerometers are supplied to the pilot's and co-pilot's displays, respectively, (mounted on the glare shield) with a display gain of  $\pm 0.2g$  full scale. All three axes are recorded on a Heiland recorder. Electrical power is provided from the aircraft 28VDC bus and is protected by a circuit breaker located on the main circuit breaker panel.

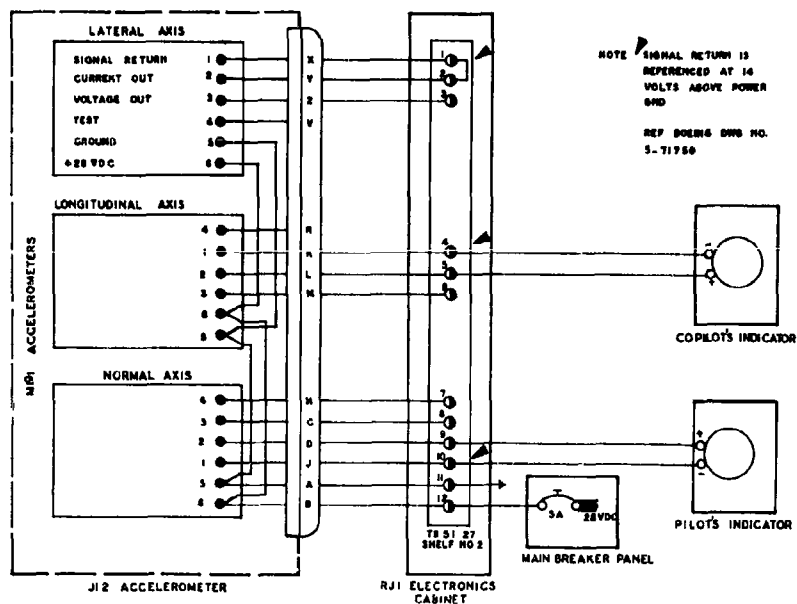


Figure 7. Wiring Diagram - Accelerometer Installation, KC-135

### C. CLOSED CIRCUIT TELEVISION

A Kintel Model 1986 ACU closed circuit television system was installed in both aircraft to be used to monitor floating objects. The system was used extensively in the KC-135 aircraft and was placed temporarily in the C-131 for evaluation. The closed circuit TV consists of a TV camera mounted forward of the float compartment viewing aft along the longitudinal aircraft axis into the float area. The electronic components are located amidships with a TV monitor in the pilot's panel. The pilot enters the zero-g maneuver while referring to his mechanical g-meter, airspeed indicator and gyro-horizon and then, when entering zero-gravity, transitions to the TV monitor which shows the floating object. The pilot flies the aircraft about the floating object to prevent impact of the object with the float compartment walls. This arrangement has enabled an increase of two to five seconds in the impact-free time. The pilot was usually able to apply only one or two impact-preventing corrections. Results of a typical set of float runs utilizing the closed circuit TV are described in Reference 13. Average total weightless time per parabola for a floating man-size package was 11 seconds. Average free float period was 4 seconds, with a maximum of 8 seconds. The system did not work successfully when installed in the C-131 because of an inadequate aircraft electrical power supply which caused a faulty synchronization of the picture. The TV monitor is shown in Figure 8 as mounted in the C-131B.

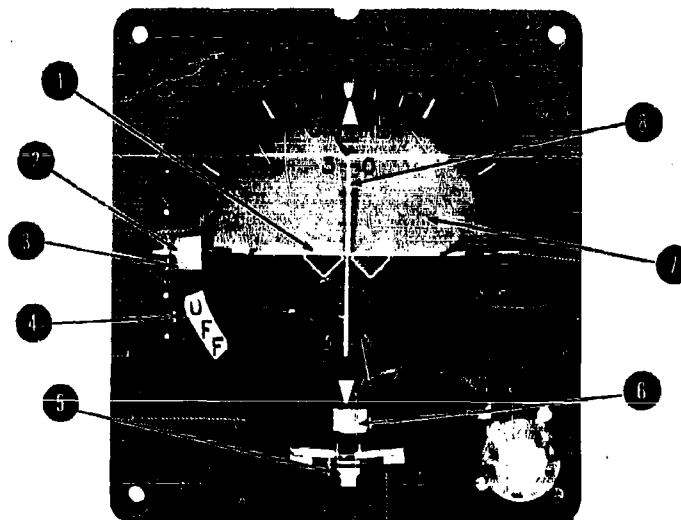
A microammeter is mounted directly above and to the right of the TV monitor. This ammeter is adjusted to give a normal acceleration indication with a sensitivity of  $\pm 0.2g$ /full scale deflection, and is used in conjunction with the TV to keep the aircraft on a nominal zero-g trajectory.



Figure 8. Closed Circuit T.V. Installation, C-131B

D. REVISION B A.D.I. MODIFICATION (C-131B)

The "Revision B A.D.I. Modification" is the basic integrated instrument system being flown and evaluated on C-131B aircraft, Serial Number 53-7806. The name stems from a modification of the basic Attitude Director Indicator system which was a preliminary attempt to provide the pilot with an integrated display of all the control information necessary to fly the zero-gravity maneuver. The basic system was a Lear Attitude Director Indicator with a standard face (Figure 9) displaying a pitch and roll sphere, horizontal and vertical director needles, a "bug" or displacement pointer on a vertical scale, turn and bank indicator, and alarm flags. This instrument varies from the standard model in that it has a modified pitch presentation.



- |    |                               |
|----|-------------------------------|
| 1. | HORIZONTAL DIRECTOR NEEDLE    |
| 2. | DISPLACEMENT POINTER (BUG)    |
| 3. | GLIDE SLOPE FLAG              |
| 4. | POWER FLAG                    |
| 5. | RATE OF TURN NEEDLE           |
| 6. | LOCALIZER FLAG                |
| 7. | SPHERE                        |
| 8. | VERTICAL DISPLACEMENT POINTER |

Figure 9. Attitude Director Indicator

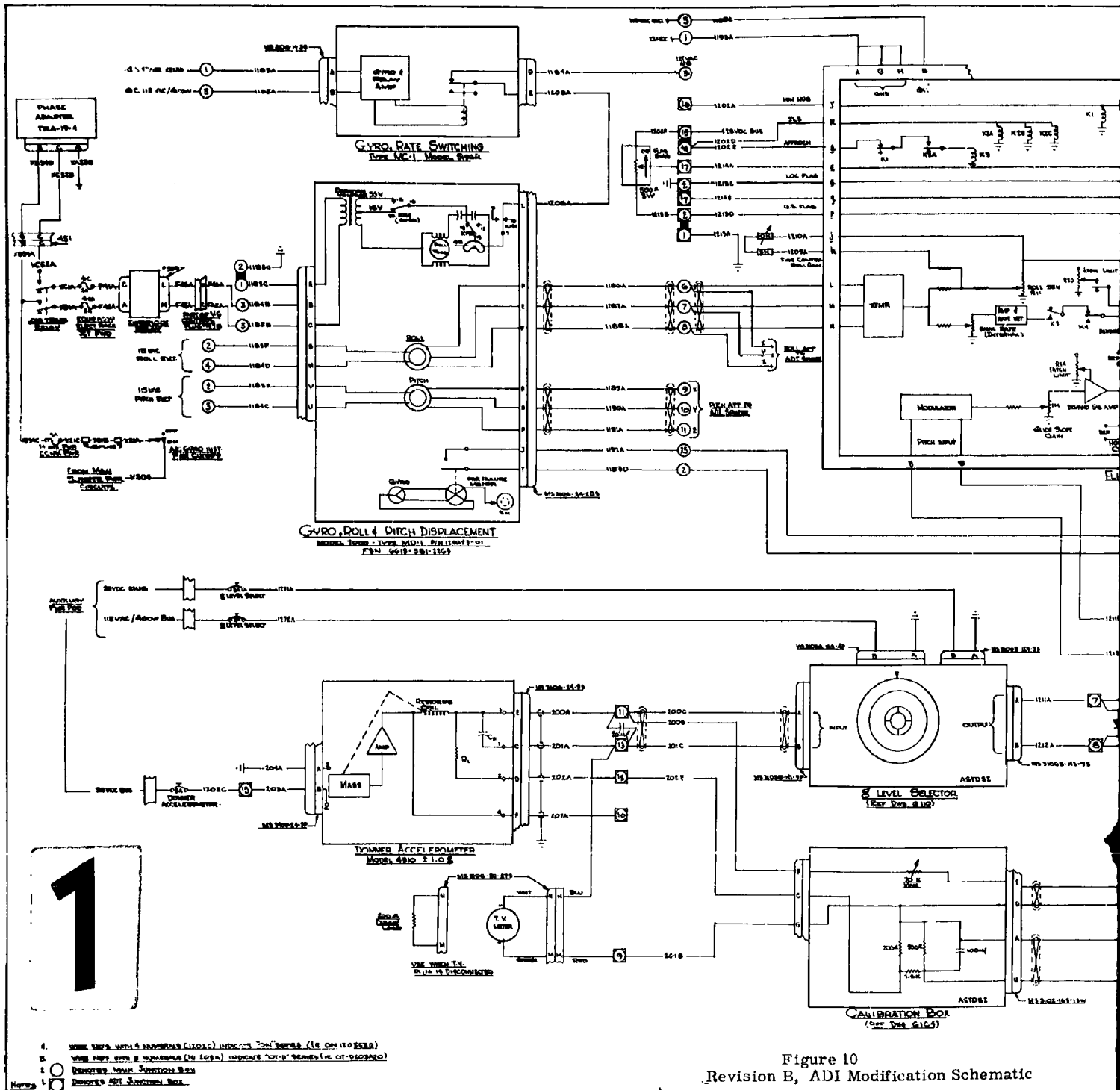


Figure 10  
Revision B, ADI Modification Schematic

1

- 4. When used with 4 switches (logic) indicate "on" status (ie. on (0055))
- 5. When used with 8 switches (logic) indicate "on" status (ie. on (0055))
- 6. When used with 16 switches (logic) indicate "on" status (ie. on (0055))
- 7. When used with 32 switches (logic) indicate "on" status (ie. on (0055))
- 8. When used with 64 switches (logic) indicate "on" status (ie. on (0055))
- 9. When used with 128 switches (logic) indicate "on" status (ie. on (0055))
- 10. When used with 256 switches (logic) indicate "on" status (ie. on (0055))
- 11. When used with 512 switches (logic) indicate "on" status (ie. on (0055))
- 12. When used with 1024 switches (logic) indicate "on" status (ie. on (0055))
- 13. When used with 2048 switches (logic) indicate "on" status (ie. on (0055))
- 14. When used with 4096 switches (logic) indicate "on" status (ie. on (0055))
- 15. When used with 8192 switches (logic) indicate "on" status (ie. on (0055))
- 16. When used with 16384 switches (logic) indicate "on" status (ie. on (0055))
- 17. When used with 32768 switches (logic) indicate "on" status (ie. on (0055))
- 18. When used with 65536 switches (logic) indicate "on" status (ie. on (0055))
- 19. When used with 131072 switches (logic) indicate "on" status (ie. on (0055))
- 20. When used with 262144 switches (logic) indicate "on" status (ie. on (0055))
- 21. When used with 524288 switches (logic) indicate "on" status (ie. on (0055))
- 22. When used with 1048576 switches (logic) indicate "on" status (ie. on (0055))
- 23. When used with 2097152 switches (logic) indicate "on" status (ie. on (0055))
- 24. When used with 4194304 switches (logic) indicate "on" status (ie. on (0055))
- 25. When used with 8388608 switches (logic) indicate "on" status (ie. on (0055))
- 26. When used with 16777216 switches (logic) indicate "on" status (ie. on (0055))
- 27. When used with 33554432 switches (logic) indicate "on" status (ie. on (0055))
- 28. When used with 67108864 switches (logic) indicate "on" status (ie. on (0055))
- 29. When used with 134217728 switches (logic) indicate "on" status (ie. on (0055))
- 30. When used with 268435456 switches (logic) indicate "on" status (ie. on (0055))
- 31. When used with 536870912 switches (logic) indicate "on" status (ie. on (0055))
- 32. When used with 1073741824 switches (logic) indicate "on" status (ie. on (0055))
- 33. When used with 2147483648 switches (logic) indicate "on" status (ie. on (0055))
- 34. When used with 4294967296 switches (logic) indicate "on" status (ie. on (0055))
- 35. When used with 8589934592 switches (logic) indicate "on" status (ie. on (0055))
- 36. When used with 17179869184 switches (logic) indicate "on" status (ie. on (0055))
- 37. When used with 34359738368 switches (logic) indicate "on" status (ie. on (0055))
- 38. When used with 68719476736 switches (logic) indicate "on" status (ie. on (0055))
- 39. When used with 137438953472 switches (logic) indicate "on" status (ie. on (0055))
- 40. When used with 274877906944 switches (logic) indicate "on" status (ie. on (0055))
- 41. When used with 549755813888 switches (logic) indicate "on" status (ie. on (0055))
- 42. When used with 1099511627776 switches (logic) indicate "on" status (ie. on (0055))
- 43. When used with 2199023255552 switches (logic) indicate "on" status (ie. on (0055))
- 44. When used with 4398046511104 switches (logic) indicate "on" status (ie. on (0055))
- 45. When used with 8796093022208 switches (logic) indicate "on" status (ie. on (0055))
- 46. When used with 17592186044416 switches (logic) indicate "on" status (ie. on (0055))
- 47. When used with 35184372088832 switches (logic) indicate "on" status (ie. on (0055))
- 48. When used with 70368744177664 switches (logic) indicate "on" status (ie. on (0055))
- 49. When used with 140737488355328 switches (logic) indicate "on" status (ie. on (0055))
- 50. When used with 281474976710656 switches (logic) indicate "on" status (ie. on (0055))
- 51. When used with 562949953421312 switches (logic) indicate "on" status (ie. on (0055))
- 52. When used with 1125899906842624 switches (logic) indicate "on" status (ie. on (0055))
- 53. When used with 2251799813685248 switches (logic) indicate "on" status (ie. on (0055))
- 54. When used with 4503599627370496 switches (logic) indicate "on" status (ie. on (0055))
- 55. When used with 9007199254740992 switches (logic) indicate "on" status (ie. on (0055))
- 56. When used with 18014398509481984 switches (logic) indicate "on" status (ie. on (0055))
- 57. When used with 36028797018963968 switches (logic) indicate "on" status (ie. on (0055))
- 58. When used with 72057594037927936 switches (logic) indicate "on" status (ie. on (0055))
- 59. When used with 144115188075855872 switches (logic) indicate "on" status (ie. on (0055))
- 60. When used with 288230376151711744 switches (logic) indicate "on" status (ie. on (0055))
- 61. When used with 576460752303423488 switches (logic) indicate "on" status (ie. on (0055))
- 62. When used with 1152921504606846976 switches (logic) indicate "on" status (ie. on (0055))
- 63. When used with 2305843009213693952 switches (logic) indicate "on" status (ie. on (0055))
- 64. When used with 4611686018427387904 switches (logic) indicate "on" status (ie. on (0055))
- 65. When used with 9223372036854775808 switches (logic) indicate "on" status (ie. on (0055))
- 66. When used with 18446744073709551616 switches (logic) indicate "on" status (ie. on (0055))
- 67. When used with 36893488147419103232 switches (logic) indicate "on" status (ie. on (0055))
- 68. When used with 73786976294838206464 switches (logic) indicate "on" status (ie. on (0055))
- 69. When used with 147573952589676412928 switches (logic) indicate "on" status (ie. on (0055))
- 70. When used with 295147905179352825856 switches (logic) indicate "on" status (ie. on (0055))
- 71. When used with 590295810358705651712 switches (logic) indicate "on" status (ie. on (0055))
- 72. When used with 1180591620717411303424 switches (logic) indicate "on" status (ie. on (0055))
- 73. When used with 2361183241434822606848 switches (logic) indicate "on" status (ie. on (0055))
- 74. When used with 4722366482869645213696 switches (logic) indicate "on" status (ie. on (0055))
- 75. When used with 9444732965739290427392 switches (logic) indicate "on" status (ie. on (0055))
- 76. When used with 18889465931478580854784 switches (logic) indicate "on" status (ie. on (0055))
- 77. When used with 3777893186295716170944 switches (logic) indicate "on" status (ie. on (0055))
- 78. When used with 7555786372591432341888 switches (logic) indicate "on" status (ie. on (0055))
- 79. When used with 15111572745182864683776 switches (logic) indicate "on" status (ie. on (0055))
- 80. When used with 30223145490365729375552 switches (logic) indicate "on" status (ie. on (0055))
- 81. When used with 60446290980731458751104 switches (logic) indicate "on" status (ie. on (0055))
- 82. When used with 120892581961462917502208 switches (logic) indicate "on" status (ie. on (0055))
- 83. When used with 241785163922925835004416 switches (logic) indicate "on" status (ie. on (0055))
- 84. When used with 483570327845851670008832 switches (logic) indicate "on" status (ie. on (0055))
- 85. When used with 967140655691703340017664 switches (logic) indicate "on" status (ie. on (0055))
- 86. When used with 1934281311383406680035328 switches (logic) indicate "on" status (ie. on (0055))
- 87. When used with 3868562622766813360070656 switches (logic) indicate "on" status (ie. on (0055))
- 88. When used with 7737125245533626720141312 switches (logic) indicate "on" status (ie. on (0055))
- 89. When used with 15474250491067253440282624 switches (logic) indicate "on" status (ie. on (0055))
- 90. When used with 30948500982134506880565248 switches (logic) indicate "on" status (ie. on (0055))
- 91. When used with 61897001964269013761131488 switches (logic) indicate "on" status (ie. on (0055))
- 92. When used with 12379400392853802752226976 switches (logic) indicate "on" status (ie. on (0055))
- 93. When used with 24758800785707605504453952 switches (logic) indicate "on" status (ie. on (0055))
- 94. When used with 49517601571415211008907904 switches (logic) indicate "on" status (ie. on (0055))
- 95. When used with 9903520314283042201715808 switches (logic) indicate "on" status (ie. on (0055))
- 96. When used with 19807040628566084403431616 switches (logic) indicate "on" status (ie. on (0055))
- 97. When used with 39614081257132168806863232 switches (logic) indicate "on" status (ie. on (0055))
- 98. When used with 79228162514264337613726464 switches (logic) indicate "on" status (ie. on (0055))
- 99. When used with 158456325028528675227452928 switches (logic) indicate "on" status (ie. on (0055))
- 100. When used with 316912650057057350454905856 switches (logic) indicate "on" status (ie. on (0055))
- 101. When used with 633825300114114700909811712 switches (logic) indicate "on" status (ie. on (0055))
- 102. When used with 12676506002282294018196224384 switches (logic) indicate "on" status (ie. on (0055))
- 103. When used with 25353012004564588036392447744 switches (logic) indicate "on" status (ie. on (0055))
- 104. When used with 50706024009129176072784895488 switches (logic) indicate "on" status (ie. on (0055))
- 105. When used with 101412048018258352145569790976 switches (logic) indicate "on" status (ie. on (0055))
- 106. When used with 202824096036516704291139581952 switches (logic) indicate "on" status (ie. on (0055))
- 107. When used with 405648192073033408582279163904 switches (logic) indicate "on" status (ie. on (0055))
- 108. When used with 811296384146066817164558327808 switches (logic) indicate "on" status (ie. on (0055))
- 109. When used with 162259276833213363428911665616 switches (logic) indicate "on" status (ie. on (0055))
- 110. When used with 324518553666426726857823331232 switches (logic) indicate "on" status (ie. on (0055))
- 111. When used with 649037107332853453715646662464 switches (logic) indicate "on" status (ie. on (0055))
- 112. When used with 1298074214657069007431293324928 switches (logic) indicate "on" status (ie. on (0055))
- 113. When used with 2596148429314138014862586649856 switches (logic) indicate "on" status (ie. on (0055))
- 114. When used with 5192296858628276029725173299712 switches (logic) indicate "on" status (ie. on (0055))
- 115. When used with 10384593717256552059450345919424 switches (logic) indicate "on" status (ie. on (0055))
- 116. When used with 207691874345131041189006918398464 switches (logic) indicate "on" status (ie. on (0055))
- 117. When used with 415383748690262082378013837597312 switches (logic) indicate "on" status (ie. on (0055))
- 118. When used with 830767497380524164756027675194624 switches (logic) indicate "on" status (ie. on (0055))
- 119. When used with 1661534994761048329512055350389248 switches (logic) indicate "on" status (ie. on (0055))
- 120. When used with 332306998952209665902411070077856 switches (logic) indicate "on" status (ie. on (0055))
- 121. When used with 664613997904419331804822140155712 switches (logic) indicate "on" status (ie. on (0055))
- 122. When used with 1329227995808838663609644282311424 switches (logic) indicate "on" status (ie. on (0055))
- 123. When used with 2658455991617677327219288564622848 switches (logic) indicate "on" status (ie. on (0055))
- 124. When used with 5316911983235354654438577129245696 switches (logic) indicate "on" status (ie. on (0055))
- 125. When used with 1063382396647070930887715448849152 switches (logic) indicate "on" status (ie. on (0055))
- 126. When used with 212676479329414186177543519769792 switches (logic) indicate "on" status (ie. on (0055))
- 127. When used with 425352958658828372355087039539584 switches (logic) indicate "on" status (ie. on (0055))
- 128. When used with 850705917317656744710174079079168 switches (logic) indicate "on" status (ie. on (0055))
- 129. When used with 1701411834635313489420348158158336 switches (logic) indicate "on" status (ie. on (0055))
- 130. When used with 3402823669270626978840696366316672 switches (logic) indicate "on" status (ie. on (0055))
- 131. When used with 6805647338541253957681392732633344 switches (logic) indicate "on" status (ie. on (0055))
- 132. When used with 13611294677082507915362784665266688 switches (logic) indicate "on" status (ie. on (0055))
- 133. When used with 2722258935176501583072556933053376 switches (logic) indicate "on" status (ie. on (0055))
- 134. When used with 54445178703530031661451138661066752 switches (logic) indicate "on" status (ie. on (0055))
- 135. When used with 1088903574070600632229022773221344 switches (logic) indicate "on" status (ie. on (0055))
- 136. When used with 2177807148141201264458045546442688 switches (logic) indicate "on" status (ie. on (0055))
- 137. When used with 4355614296282402528916091092885376 switches (logic) indicate "on" status (ie.

Date	Revision	By	Check

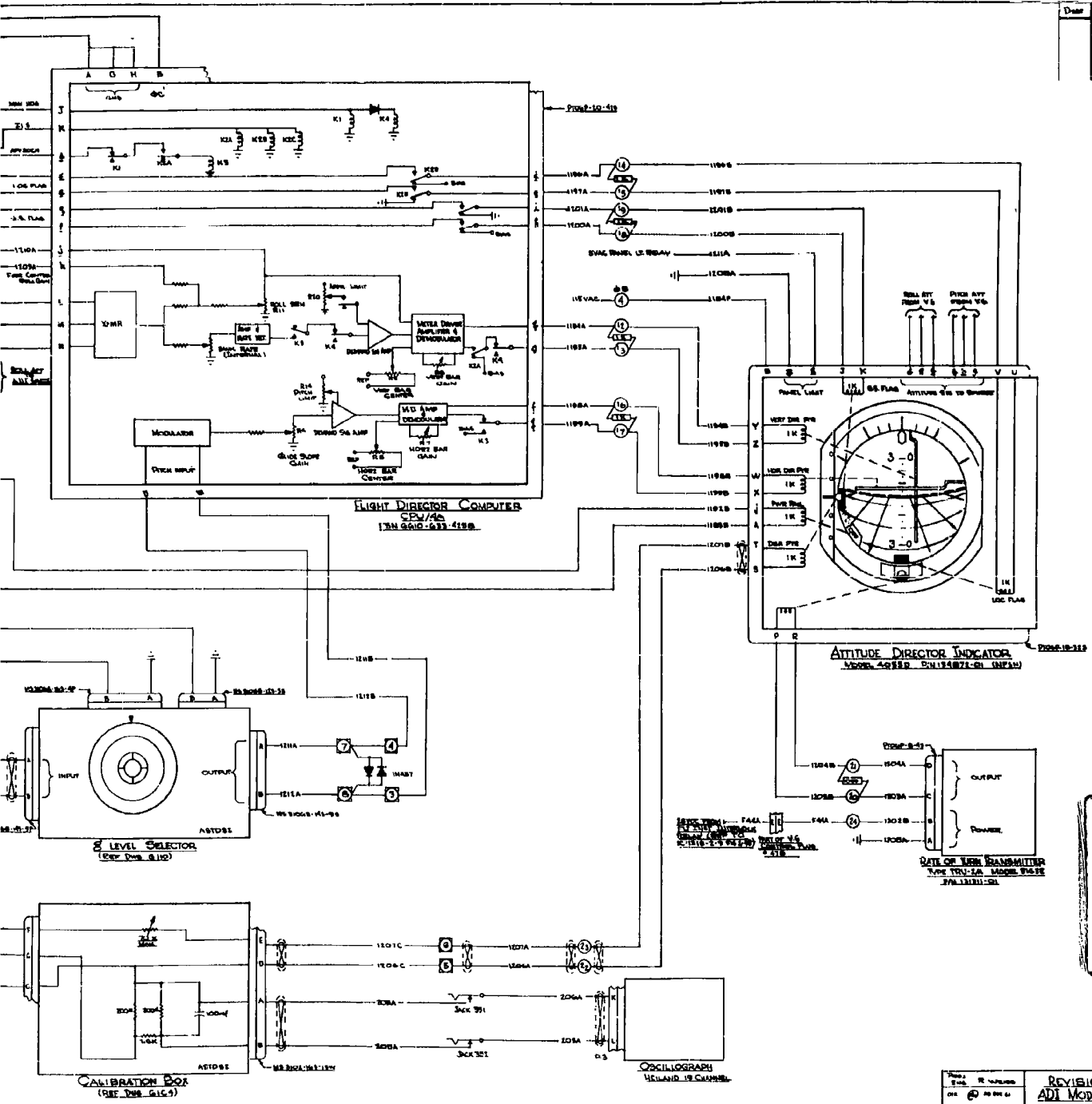


Figure 10  
B, ADI Modification Schematic

Rev.	By	Checked	DATE	REVISION	DATE

**REVISION B**  
**ADI MODIFICATION**

3 Dwg No G 111

The original modification to the standard A.D.I. system consisted of displaying the roll gyroscope signal on the vertical director needle and displaying the normal acceleration signal from a Donner Model 4310 Linear Servo Accelerometer on the displacement pointer (bug). This system flew successfully for approximately six months, and was then again modified into what is now called the "Revision B A.D.I. Modification" with the addition of a G-Level Selector, closed circuit television provisions, the use of the horizontal director needle for pilot commands, and a centralized junction box which permits changes to the system with minimum disruption of flight schedules and aircraft wiring. A description of the system follows: Reference should be made to Figure 10 which is a combination block diagram and schematic of the system.

The Attitude Director Indicator system is a standard ADI system utilizing the Lear Model 4055D Indicator, Type CPU-4/A Flight Director Computer, Type MD-1 Switching Gyroscope, and the Type TRU-2/A Rate of Turn Transmitter. The instrument panel is shown in Figure 11 and the equipment installation in Figure 12. The signal circuits from the pitch and roll gyroscope to the horizon sphere in the indicator are standard, as are the turn and bank indication and flag circuits. Gyroscope roll erection is disconnected during turns to prevent undesirable gyro erection to a false vertical. The Flight Director Computer was operated in the Manual Heading mode, which provided the proper flag bias to retract the instrument flags. The modifications to the standard ADI system involved placing a normal accelerometer signal (accelerometer installation is shown in Figure 13) on the displacement pointer and displaying the roll gyroscope output on the vertical director needle with a gain of 3/4" deflection per degree of roll of a "fly-to" sensing. The purpose of this signal was to give the pilot a sensitive roll angle indication to facilitate his keeping the wings level during the large aircraft trim changes which occur during the parabola. The Calibration Box shown in Figure 14 was used to calibrate the recorded accelerometer signal, as well as to provide a means of adjusting the displacement pointer gain. This system, as described above, constituted the "ADI Modification" for zero-g flight.

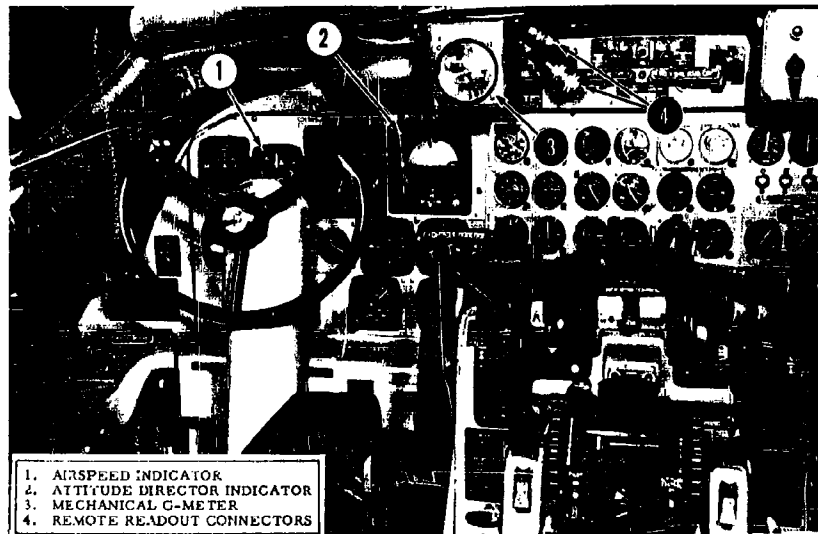


Figure 11. Pilot's Panel - ADI Modification



Figure 12. ADI Modification  
Instrument Installation

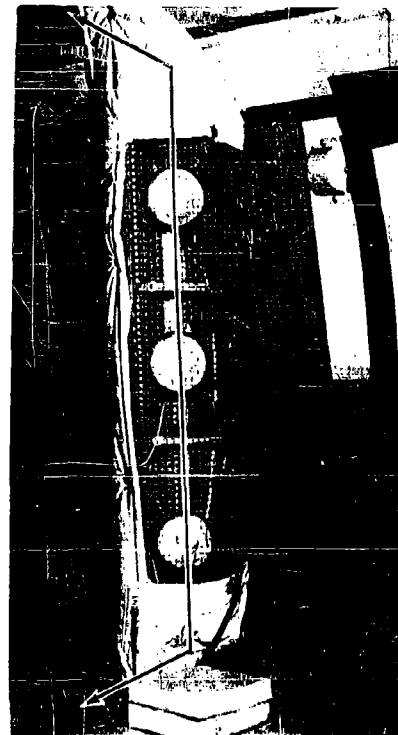


Figure 13. Donner Accelerometer  
Installation

The major additions to the "ADI Modification" which make up the "Revision B ADI Modification" were the addition of the G-Level Selector and Isolation Amplifier, the wiring provisions for the closed circuit television meter, the accelerometer damping capacitor, revised Flight Director Computer switching arrangement and flag biasing, and use of the horizontal director needle of the ADI. A detailed description of the revised system follows, with design details on the non-standard parts of the system. The standard parts of the ADI system are described in the appropriate Air Force Specifications and Technical Orders, and will not be repeated here. (References 4-7 give relevant Air Force Technical Orders).

Referring again to Figure 10, one can follow the normal acceleration signal through the system to its indicator and recorder outputs. The accelerometer used is a force-balance linear servo accelerometer Model 4310 (Donner Scientific Division of Systron Corporation). Technical data on this accelerometer appears in Appendix B. The accelerometer provides two outputs - a voltage output of  $\pm 7.5$  VDC about a 14 VDC reference for full scale acceleration ( $\pm 1g$ ) and a current output of  $\pm 1.4$  ma for full scale acceleration

The accelerometer is mounted on the floor of the aircraft in the middle of the float area (Figure 13) with its sensitive axis roughly coincident with the aircraft normal axis. The actual sensing of the accelerometer is in a negative sense, that is, minus voltage output for aircraft positive normal acceleration. This arrangement was necessitated by an undesirable recovery characteristic of the accelerometer for positive acceleration overloads. The accelerometer range of  $\pm 1.0/g$  is exceeded by 250% during the pull-up and pull-out maneuvers. The mass pickoff mechanism is so constructed that two flat plates bathed in a damping fluid come into sudden contact during the maneuver for positive acceleration. Upon recovery from this overload, a sticking of the two plates occurs, giving a delay between one to eight seconds before output returns to normal. This problem was overcome by inverting the accelerometer so that it is subject to a negative overload, where the mass strikes an overload stop, but does not stick upon recovery. The voltage output at Terminal 3 with respect to Terminal 1 of the accelerometer feeds into the G-Level Selector and Operational Amplifier. Here it is subtracted from a g-level bias, and the limited error signal is modulated by the Flight Director Computer (FDC) glide slope input modulator. The modulated signal is scaled, amplified and limited, and is further amplified by the meter amplifier of the FDC.

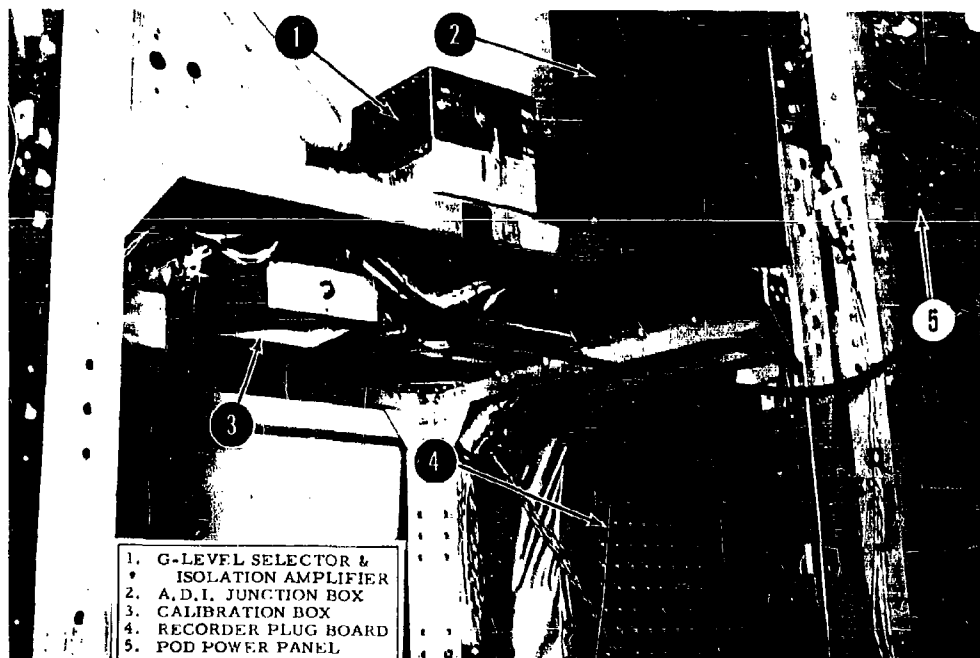


Figure 14. Control Rack R-7,  
Revision B ADI Modification

Relays K2A, K2B, K2C and K3 are energized in the zero-g parabola mode by means of 28 VDC from the aircraft supply on the ILS and APPROACH switching inputs of the FDC. The acceleration signal powers the Horizontal Director Needle of the ADI, which has an external 1 kilohm resistor shunt for impedance matching. The result of this signal processing is to display, on the Horizontal Director of the ADI, a signal proportional to the difference between commanded and actual aircraft normal acceleration. Phasing is an upward bug deflection for positive acceleration. The limiting diodes at the output of the G-Level Selector enable the supplying of its output, in the case of a malfunctioning Flight Director Computer (FDC), directly to the Displacement Pointer (bug) of the ADI. This may be accomplished by a simple switch of wires in the ADI Junction Box. The diodes act as current limiters to prevent damaging of the bug meter coil. The diode limiter characteristic appears in Figure 15. The gain of the G-Level Selector is set so that proper bug deflections are obtained. Since the sensitivity of the Horizontal Director needle movement is approximately a tenth that of the bug, a gain of ten must be picked up in the FDC when it is used.

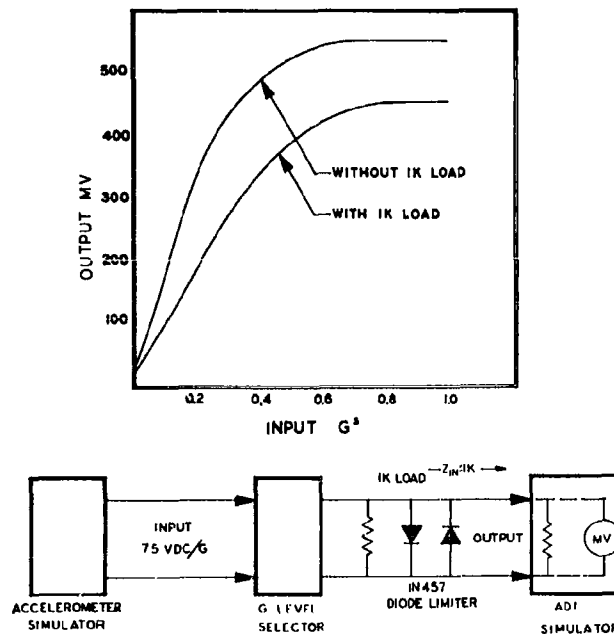


Figure 15. Diode Limiter Transfer Characteristic

An explanation of the G-Level Selector and Isolation Amplifier operation follows: The Selector installation is shown in Figure 16 and the schematic in Figure 17. The G-Level Selector consists basically of a cathode coupled balanced-bridge differential amplifier with the accelerometer signal fed into one grid and the command g-level fed into the other. Output is taken off the cathodes of the two triode sections in a differential manner, scaled with a series potentiometer, and leaves through the two pin output connector.



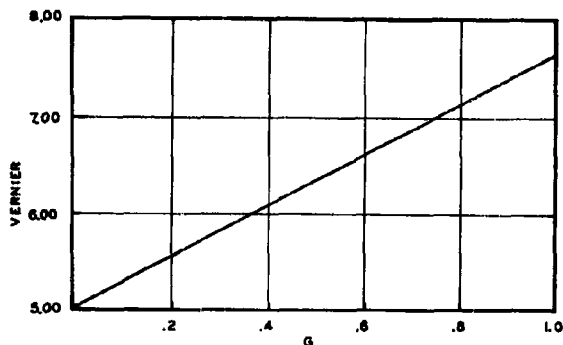


Figure 18. G-Level Selector Vernier Setting Vs. G Level

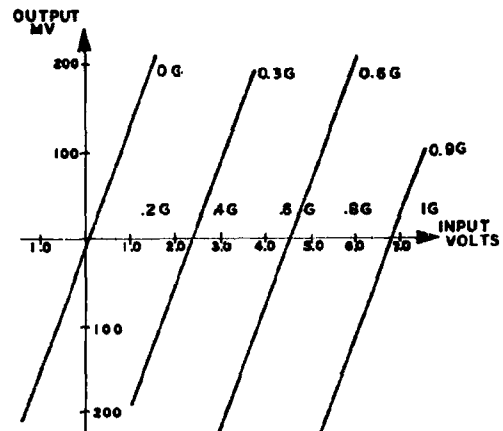


Figure 19. G-Level Selector Transfer Characteristic

The G-Level Selector and Isolation Amplifier has three controls on the front face and two adjustments on the right side of the unit (viewed from the front panel). The ON-OFF switch left of center on the front face controls the power and bias supplies of the amplifier. When this switch is in the OFF position, the unit is completely dead. The OUTPUT ON-OFF Switch to the right of center on the front face disconnects the amplifier output from the external load and connects the accelerometer input to the amplifier output terminals, thus bypassing the amplifier completely. In the middle of the front panel is a vernier potentiometer which is the G-Level Selector. This control provides the variable bias to grid 2 of the amplifier. The scale marking is arbitrary and goes from zero (zero volts) to 10.0 (28 volts). Vernier setting versus desired g-level is shown in Figure 18. This chart is based upon an accelerometer output of minus 7.5 volts to plus 7.5 volts for a -1g to 1g field. If it is desired to use the unit with an accelerometer with a different output, this may be done quite easily with a recalibration of the vernier. The sensitivity and centering of the unit are adjusted at initial system calibration.

Calibration of the system is accomplished with an Accelerometer Signal Simulator. A schematic diagram of the Simulator is shown as Figure 20, and the simulator in use is pictured in Figure 21. The simulator consists of an adjustable voltage source about an adjustable bias level. A meter monitors the simulator voltage for direct reading. The output impedance of the simulator of 5000 ohms correctly simulates the output impedance of the accelerometer. The excitation for the Simulator is the 28 VDC aircraft supply, and all connections can be made in the ADI Junction Box. The wiring is complete in the unit, and no separate leads or clips are necessary.

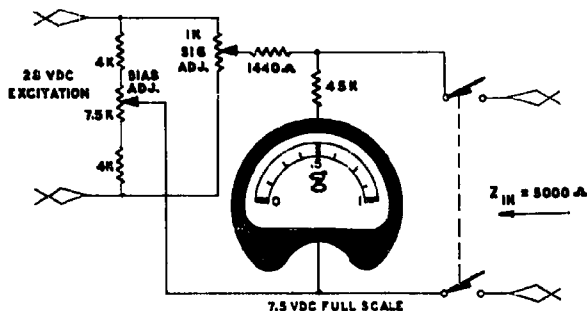


Figure 20. Accelerometer Signal Simulator - Schematic

Recording of the normal acceleration signal from the accelerometer is performed using the current output connections of the accelerometer. In series with the T.V. meter, which is described in Section II-C, is a compensation and gain network located in the Calibration Box. The Calibration Box may be seen mounted on Equipment rack R-7 in Figure 11. This compensation network scales and filters the acceleration signal. The recorder signal is then lead through a pair of shielded plug leads into the recorder junction box, where it is distributed to one channel of a 24 channel Heiland light-beam galvanometer recorder. Recording sensitivity of this trace is approximately 3.3 inches per "g".

In use, the accelerometer and G-Level Selector are connected with a zero-center microammeter placed in the reference voltage leg (at Terminal 13 of the ADI Junction Box). The bias centering control of the G-Level Selector is adjusted until the microammeter is nulled. This assures that the two units operate about the same reference. The accelerometer leads are then removed from terminals 11 and 13 of the ADI Junction Box and the accelerometer simulator output leads clipped on in their place. The bias center control on the Accelerometer Signal Simulator is then adjusted to zero the microammeter in the reference leg. The Simulator is then used to produce calibrating voltages which are monitored at the ADI.

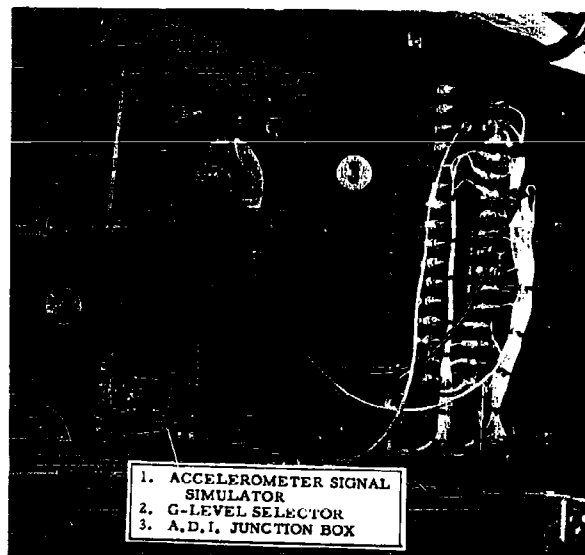


Figure 21. Accelerometer Simulator In Use

The last element in the Revision B A.D.I. System is the presentation of a standby acceleration signal for the pilot on the ADI bug. This signal is scaled by means of a series potentiometer in the Calibration Box with full-scale deflection of the bug (+ 2 dots) representing full-range normal acceleration (+ 1g). This is used by the pilot as a rough check on g-level, as well as a backup indicator in case of failure of the G-Level Selector or the Flight Director Computer. Sensitivity of this indication may be varied easily by means of the scaling potentiometer.

### SECTION III - TESTS PERFORMED

#### A. LEVEL OF ACCURACY AND MEASURES OF GOODNESS

A description of a typical normal acceleration signal recording (Figure 22) aids in understanding the instrumentation and data reduction. The area of interest is that time between the termination of the 2-1/2 g entry pullup and the beginning of the 2-1/2 g recovery pullout. The shape of the steep part of the curve at the left is the discharging time constant of the external 20 uf damping capacitor across the output of the accelerometer and is not a true indication of normal acceleration during that period. As soon as the indicator settles (for those runs using the Donner Accelerometer as a basic reference), the pilot initiates a control motion. This causes an initial overshoot and then ultimate damping out about the control value. Two of the measures used in evaluation of the accuracy of the parabola are the "initial overshoot" at the beginning of the parabola before it settles, and the "maximum error," which is measured somewhere between the time the response settles and time of pullout. In Figure 22, a deviation labeled "tuck" is shown towards the end of the parabola. This characteristic appears on many of the traces and is sometimes extremely pronounced. It results from an aerodynamic characteristic of the aircraft in the particular zero-g flight regime and is felt as a tendency to "tuck the nose under".

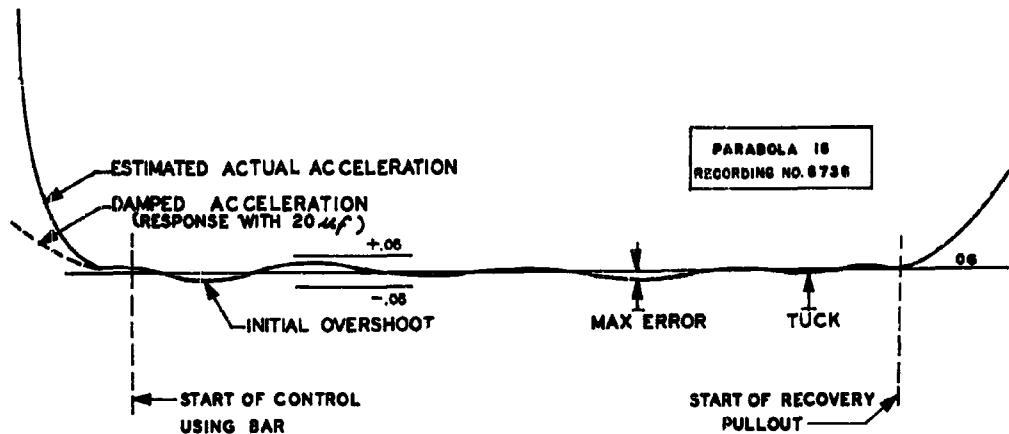


Figure 22. Typical Parabola - Significant Points

The actual "measure of goodness" chosen to evaluate results of this program is the time within a given tolerance band. This concept is illustrated in Figure 23. In applying this measure, it is necessary to choose a band width which will make the results significant when it is applied to the data. In the beginning of this evaluation, a "time within 0.02 g" (T02) was chosen, but it was found that this did not yield very significant results, and that wider and narrower bands should be taken. The lower limit (T01) is based upon the readability and trace width of the recording, while the widest limit (T05) is

chosen wide enough so that it includes most of the variations encountered during a typical maneuver. In some cases, if the trace contained two significant periods within a given band, with a brief time outside that band, the "time-within-the-band" was considered to be the sum of the two components. The "time" referred to is an arbitrary measure in time units and is not in "seconds". Instrumentation difficulties throughout the entire evaluation prevented establishment of a firm time base, but the runs may still be compared one against the other without reference to absolute time units. For an approximation of real time (in seconds) one may multiply the arbitrary time units by two. This was confirmed by later runs with a functioning time reference (Table 7). This data is in "seconds".

Applying the above criteria to fifty significant parabolas, the results were tabulated in Table 1 in Appendix C. Dispersion is large in the data, but the figures approximate the general level of accuracy of the parabolic maneuver. There is no data entry for "initial overshoot" for the flights of 16 October as these were tests of the G-Level Selector, and standard zero-g parabolas were not initiated. This provided no common reference point to evaluate initial overshoot.

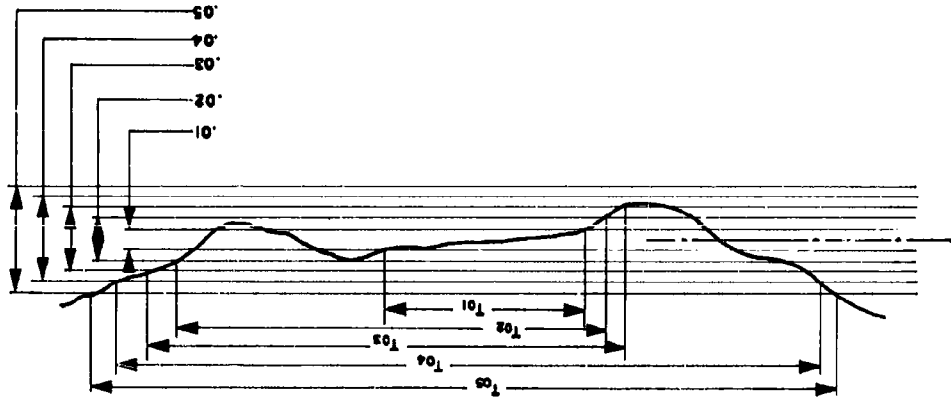


Figure 23. Diagram Illustrating "Time-Within-Tolerance"

#### B. DISPLAY GAIN VS. ACCURACY

Results of the investigation of the effect of display gain on system performance are given in Figure 24. The system, for this test, consisted of the "Revision B A.D.I. Modification". Abscissas for Figures 24, 26 and 27 are normal acceleration for two bars Director Needle displacement. Decreasing gain is plotted toward the right. It would have been desirable to run these tests through a greater range of gains, but this was the limit of capability of the G-Level Selector gain control.

Figures 24a-e present the time within the various tolerance bands for four chosen gains. The estimating equation (solid line) and the zone of scatter or standard error of estimate (dashed lines) are shown. Figure 24f presents the five estimating equations plotted for comparison. When using a wide tolerance

band, there is a tendency toward a decrease in time-within-the-band with increasing gain. For the narrower bands there is an increase in time-within-the-band for increasing gain. This may be explained in the following manner: There are two methods for the normal acceleration to exceed the limits of the tolerance band in question. It may, due to low system gain and an overdamped characteristic, wander from the control value and have reduced accuracy. It may, due to high gain and an underdamped characteristic, overshoot the control value but have good accuracy around the control point. Large variations in aerodynamic gain during the maneuver do exist. The flight regime ranges from a maximum air speed and low altitude during the pullups to almost stall speed and a higher altitude at the parabola peak. This means that the system undergoes large changes in gain (in this case, the  $\theta/\delta_e$  gain) during the parabola. This gain range, when coupled with the intentional display gain variation, gives us a system which would be expected to change its damping characteristic drastically during the maneuver. This is verified by the pilot, who notes large changes in control forces during the maneuver. If one assumes that the statements about damping and gain and their influence on the method of leaving the tolerance band are valid, then one would expect to observe that the times-within-the-tolerance-band occur around the parabola apex for high electronic gain and towards the ends of the parabola for low electronic gain. An inspection of Table 6, Appendix C, and Figure 25 shows this to be true. As a further explanation, with high electronic gain together with high aerodynamic gain, an underdamped system response occurs which causes relatively high overshoots which affect the larger tolerance bands but give tighter control about zero. On the other hand, a low aerodynamic gain coupled with a low display gain gives a "sloppy" response which degenerates the smaller tolerance band performance. This hypothesis explains the results in Figure 24f and also indicates that the best control gain for all portions of the parabola seems to be between the 0.4 and 0.3 "g" full scale on the display.

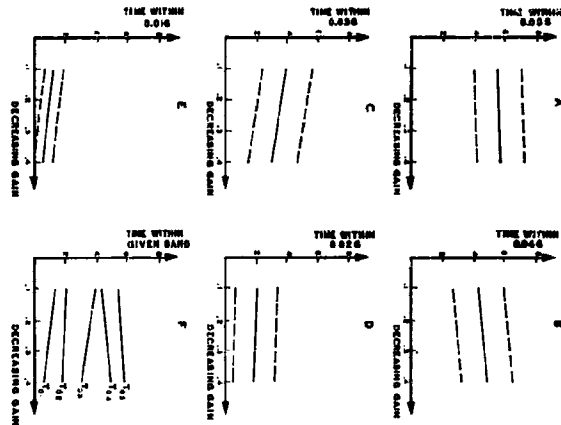


Figure 24. Time Within Tolerance Vs. Display Gain

Figure 26 shows that there is no significant variation of maximum error with gain. Figure 27 shows that the initial overshoot increases with an increase in display gain, which is to be expected. Aerodynamic gain does not affect this plot because the entry into the parabola is consistent from parabola to parabola, and only display gain varies.

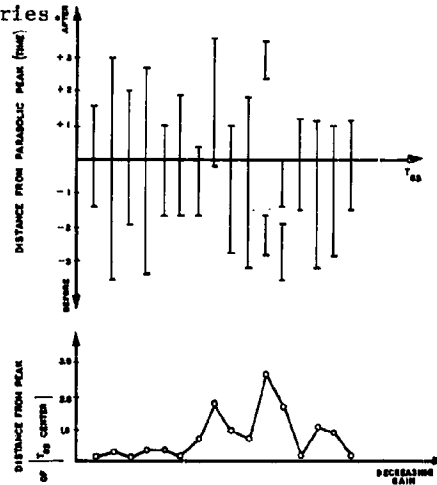


Figure 25. Distance from Parabola Apex Vs. Display Gain

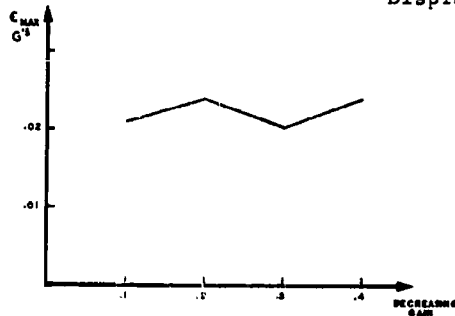


Figure 26. Maximum Error Vs. Display Gain

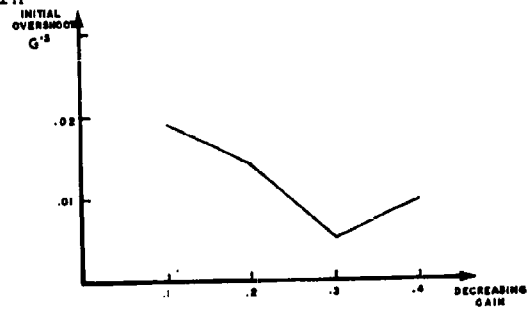


Figure 27. Initial Overshoot Vs. Display Gain

Step responses of the system (Figure 28) show the response of the pilot-display-aircraft system to step display inputs. Parabola (c) illustrates the response to steps at two different points in the same parabola. There is considerable variability of parameters within any one parabola, as is demonstrated by the range of damping exhibited by this set of step responses.

Figure 29 shows a trace chosen because of its exaggerated oscillatory characteristic. Figure 30 is a distribution of system frequencies (taken from the traces which had distinct frequencies). A distribution seems to appear about two

major frequencies of .25 and .50 (arbitrary units per second, equivalent approximately to 1/8 and 1/4 cycle per second.

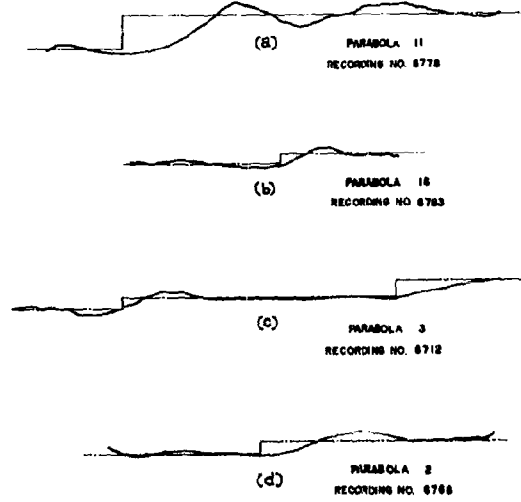


Figure 28. System Step Responses

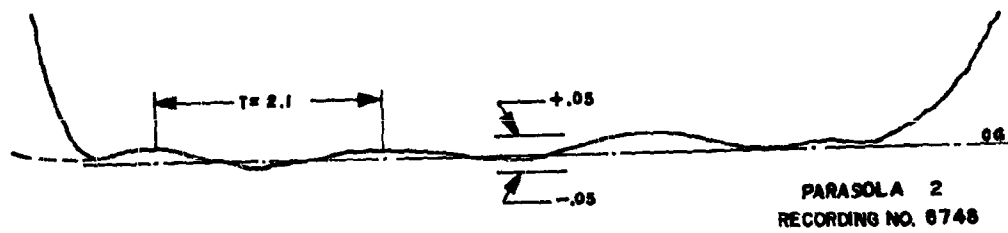
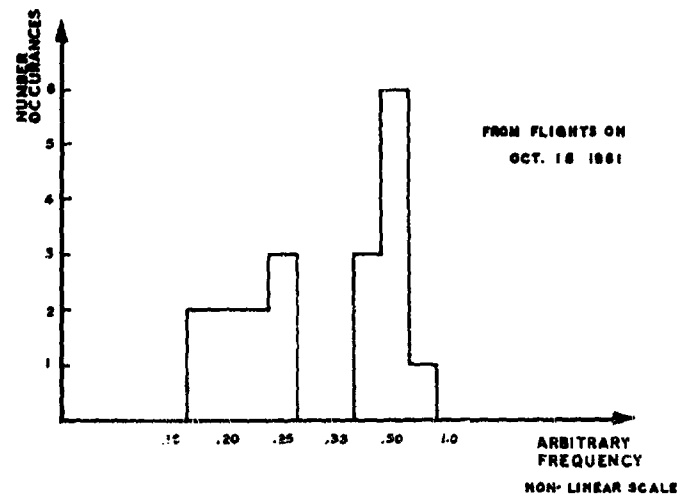


Figure 29. Trace Showing Oscillatory Characteristic

Figure 30. Histogram of System Characteristic Frequencies



C. THREE AXIS ACCELEROMETER VS. REVISION B ADI MODIFICATION SYSTEM ACCURACIES

Table 1, Appendix C shows a comparison of system performances using the Horizontal Director Needle of the A.D.I. as a basic display as opposed to the Remote Readout of the Three Axis Accelerometer Package as the basic display. The runs of 16 October, 18 October and 30 October utilized the A.D.I. as the basic pilot display. The runs of 27 October utilized the Remote Readout as a basic pilot display, and the accuracy of the parabolas on that date is significantly lower than the mean for all but the time within 0.01"g". Maximum errors were also larger, although overshoot was the same.

D. KC-135 INSTRUMENTATION ACCURACY

The results of a typical set of zero-g flights using the accelerometer instrumentation described in Section II-B and the closed circuit television described in Section II-C are tabulated in Tables 8 and 9 of Appendix C. Table 8 presents a summary of the times-within-tolerance for eleven KC-135 flights of 1961 and early 1962. Table 9 presents typical stopwatch float times for a set of flights from the same period.

Many factors influence the float time of a capsule, and good airframe performance may not be correlated with good float times. An obviously important factor is weather conditions. The pilot Flight Log contains notations when weather conditions were abnormal. Notations of air turbulence appear for 14 April 1961 and 19 February 1962. The float times for the 14 April flight are abnormally low (Table 9) and the times-within-tolerance poor for the 19 February flight. On the other hand, calm weather may enhance system performance, as seems to be the case for the 13 February morning flight.

Another important factor is the capsule size and float volume. The larger capsules demand tighter airframe control because of the shorter distance they can travel before impact. Some of the experiments early in 1961 took place in an inflated chamber within the aircraft float area. This tended to decrease the usable float space and thus yield lower float times.

The type of experiment is very important when considering float times, because test requirements sometimes dictate special flight conditions. Liquid boiling experiments, for example, may tolerate no negative accelerations. The pilot must therefore exercise extreme caution upon entering zero-gravity so as not to overshoot and approach zero-g unidirectionally. Float times in experiments in human movement sensations or soaring may be shortened significantly by improper extension of arms or legs by the subject, with resulting impact with the fuselage. The flights of 8, 12 and the afternoon flight of 13 February 1962 are examples of low float times caused by the movements of inexperienced subjects.

Another highly significant factor is the method of launching the test capsule or subject. Methods which are currently used include the "hand launch", "drop table" and "asymptotic" or "floor release". A capsule or subject which

is hand launched is stabilized by being held by two test operators until the aircraft is at zero-gravity. At this point the capsule is released, an effort being made by the "launchers" to impart a minimum velocity to the capsule. The drop table is so constructed as to "drop" from under the capsule at zero-gravity. Asymptotic, or floor launch relies upon the pilot's flying a slight negative acceleration, and thus "dropping" the aircraft away from the capsule. The errors in hand launches arise from the initial velocity and acceleration imparted to the capsule by the "launchers". The drop table and floor launches are also imperfect because they usually impart some initial force to the capsule.

A very important factor in floating capsules is pilot technique. Pilots differ from one another in their control techniques, some favoring slow continuous corrections, and others favoring quick discontinuous control motions. The flight of 20 February 1962 was flown by a pilot favoring the gradual corrections. An average T05 of 10.11 seconds yielded an average float time of 4.5 seconds. The flight of the morning of 13 February was a flight of the same type of capsule. On this flight, a T05 of 8.6 seconds yielded an average of 9.2 seconds of impact-free float time. This same pilot has produced an 18 second float time while making four airframe corrections approximately  $\pm 0.1g$ . The durations of these floats are all expressed in real time.

Fore-and-aft control of acceleration during these parabolas was generally good, yielding maximum excursions on the order of  $0.01g$ , but maximum excursions in lateral acceleration were about five times as great, indicating an area which might require some further study.

## SECTION IV - FUTURE WORK INDICATED

### A. REVISION D SYSTEM

The Revision D system is proposed as the logical extension of the already tested Revision B system. Major changes include a unified zero-gravity operator's control panel which incorporates all of the mixing, gain, and shaping circuits and self-contained testing and calibration provisions which were not used on the earlier configuration. A description of the Revision D system follows:

The control panel contains a selector switch which will enable operator selection of any of five modes of operation. These five modes are: manual flight, zero-gravity programmed flight, sub-g level select, g-decay maneuver, and super-g level select. The super-g level flight is the only one which differs significantly from the others. It is proposed that studies requiring a higher than one-g field take place in an aircraft flown in a constant-g turn. This turn will be controlled by the same indicator which is used for zero-g parabolas. An exception is that the control signal will be displayed on the vertical director needle as opposed to the zero-gravity flight where the signal is presented on the horizontal director needle. This will provide for control of normal-g by means of aileron control as opposed to elevator control.

A block diagram of the proposed Revision D system is shown in Figure 31. The acceleration and jerk reference signals will be summed in a summing amplifier with a variable bias. This variable bias is the command signal which will program the various modes of operation. For a manual zero-gravity flight, the bias will be zero. For a programmed zero-gravity flight, the entire maneuver is programmed. The program is generated by sequentially connected relays with switch points governed by air speed and pitch angle, similar to the manner in which the pilot computes switch points while flying the maneuver. For g-level selected flight (both sub- and super-g), the bias will be a fixed, other-than-zero voltage. The switching arrangements at the output of the summing amplifier will be compatible with the selected mode of operation. It was mentioned previously that all modes of operation will involve a compensatory display on the horizontal needle of the ADI with the pilot flying elevator. Super-g mode involves flying ailerons with a compensatory display on the vertical needle of the ADI. The purpose of the jerkmeter is to provide a lead term for stabilization of the closed loop pilot-display-aircraft system. The amount of this stabilizing signal will be adjustable and will be determined in future tests of the system. Another feature to be incorporated into this control panel will be a variable display compensation which will consist of lead-lag terms operating on the display error signal. The nature of this compensation will be derived from an analog simulation of the system or from in-flight evaluations. The g-decay maneuver is a maneuver which involves a gradual and linear decay of the gravity field from +1 to 0g. This maneuver will be programmed by either a motor driven potentiometer bias or by a linear electronic decay.

Test provisions will be incorporated in the control panel. There will be two meters: An input and power meter and an output and null meter.

Quantities to be metered will be selected with appropriate selector switches. These two meters will enable ground and in-flight calibration of the system and the setting of gains, scale factors, decay rate and amplifier balance. The test equipment incorporated in the panel will also include a signal simulator which will generate signals approximating those of the accelerometer, jerkmeter, and airspeed and altitude transducers. This will eliminate the necessity of loosening the accelerometer-jerkmeter mount each time a calibration of the equipment is performed. It will also enable in-flight checks by the operator to insure proper equipment operation.

Other portions of the Revision D ADI Modification will remain the same as the Revision B system.

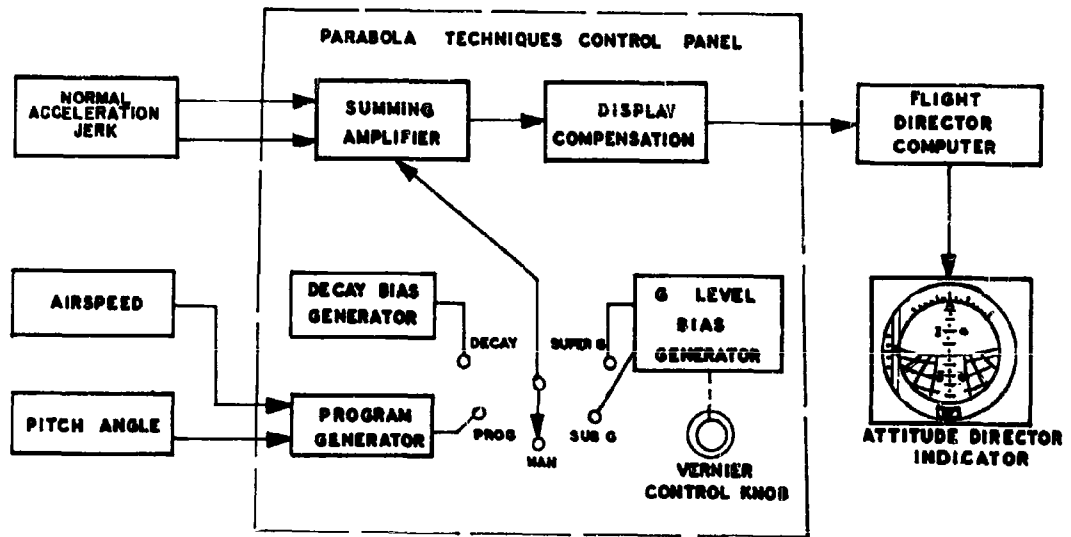


Figure 31. Proposed Revision D System Block Diagram

## B. ANALOG SIMULATION

The purpose of this simulation is to study the zero-gravity maneuver as performed with C-131B, Serial Number 53-7806, in an effort to improve the pilot's and co-pilot's displays and to optimize the flight trajectory. Improvement is defined in terms of an increase in zero-gravity time, an increase in the accuracy of the normal acceleration control, and an unburdening of the pilot during the maneuver.

The items to be studied by means of the simulation are as follows (but the study is not necessarily confined to the following aims):

1. Study quickening and other compensation methods for pilot and co-pilot displays.
2. Study the effect of display gain.
3. Evaluate and design a maneuver programmer.
4. Study the effect of thrust changes on the gravity field.
5. Study the effect of normal accelerometer longitudinal position on accuracy of the mission.
6. Optimize entry angle and pullup trajectory for a maximum zero-gravity trajectory.

A block diagram of the computer mechanization appears as Figure 32. The heart of the simulation is the Longitudinal Three Degree of Freedom Aircraft Dynamics. Formulation of the equations describing the longitudinal motions of the C-131B is based upon methods in References 8 and 10.

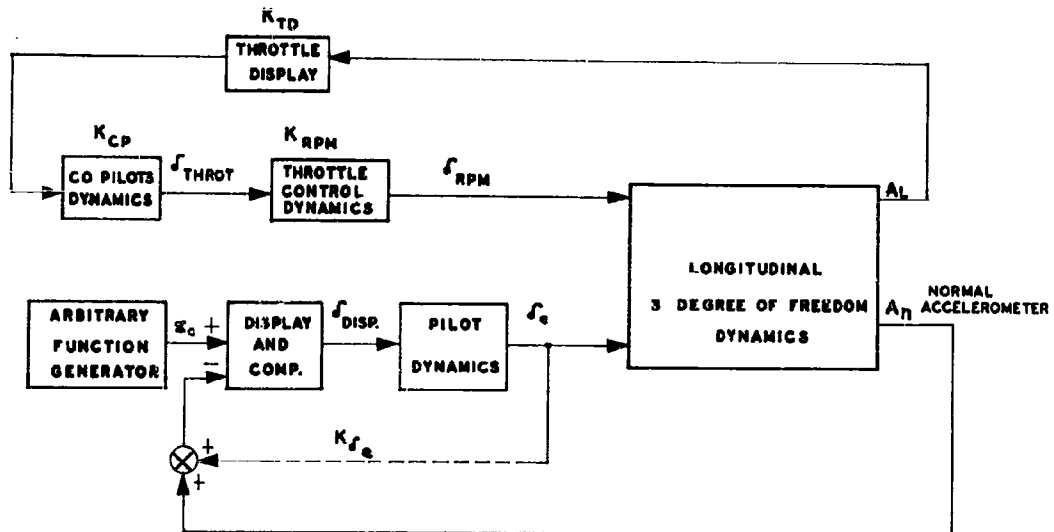


Figure 32. Analog Simulation - Block Diagram

Two control channels will be investigated: the pilot's normal acceleration (pitch) control and the co-pilot's longitudinal acceleration (throttle) control. Pilot Dynamics will be fixed in this simulation as consisting of a pilot gain, a reaction time delay, trim integration, neuromuscular lag, and a variable lead-lag. It should be noted at this point that the Pilot Dynamics is a highly uncertain quantity and that a study is advisable to determine a better approximation of the pilot transfer function in this specific task, but that this is not within the scope of the present investigation. The Display and Display Compensation are variables and are the prime object of this investigation. The Arbitrary Function Generator is to be developed in the simulation.

In the second control channel (throttle or longitudinal acceleration control), the co-pilot will be simulated as a simple gain  $K_{cp}$ , since his task is considerably simpler than that of the pilot's and the Throttle Control Dynamics contain a large enough lag to negate the co-pilot's response. The quantity  $A_L$  will include a term representing the displacement of the normal accelerometer from the center of gravity and will be used to investigate the effect of longitudinal position of the normal accelerometer.

Simulation equations have been developed in terms of aircraft body axes. Equations and their derivation may be found in Appendix D.

#### C. VARYING DISPLAY GAIN AND COMPENSATION

Future work will include a study of the effects of display gain and compensation in the various modes of operation. The display gain will be varied at the control panel, and the effect of the display gain on piloted operation will be studied. Compensation referred to here is any compensation consisting of lead and lag terms which should be put into the display to improve operation of the system. Improved operation has been defined as increased zero-gravity time within a specified tolerance band. It is anticipated that the most important compensation will be provided by the lead term of the jerkmeter, but it is possible that a lag must be generated to insure stability of the system. Other compensation terms may also be found necessary.

#### D. AUTOPILOT CONTROLLED ZERO-G

At the completion of tests investigating manually-controlled zero- and sub-gravity flights, the next logical step in the program would be to by-pass the pilot and provide for automatically controlled maneuvers. It is anticipated that the major portion of the studies of the stability of the system will have revealed certain system dynamics which will insure stable flight. These dynamics will be mechanized by means of the previously described systems and the already installed E-4 automatic pilot in the C-131B and the MC-1 automatic pilot in the KC-135. There will be some evaluation necessary after mechanization of the automatically controlled flight. The requirements will be somewhat different from those of piloted flight since the pilot has the ability to adapt his response to optimize the system, an ability not shared by the automatic pilots installed in the two aircraft. Some optimum compensation may be found which will insure satisfactory flight throughout this flight regime using automatic pilot. Portions of the automatic pilot are already being used on

zero-gravity flight in the KC-135. During the regular zero-g flight of this aircraft, the roll and yaw axis stabilization systems are being used with only the pitch axis being manually controlled by the pilot. Work to date indicates that this is a satisfactory arrangement which will somewhat unburden the pilot, but it is desirable to have completely automated flight in the future.

#### BIBLIOGRAPHY

1. Gerathewohl, S. J., Zero-G Devices and Weightlessness Simulators, Publication 781, National Academy of Sciences - National Research Council, Washington, D. C., February 1960.
2. Hammer, Lois R., Aeronautical Systems Division Studies in Weightlessness: 1959-1960, Wright Air Development Division Technical Report 60-715, Aeronautical Systems Division, Wright Patterson Air Force Base, Ohio December 1961.
3. Difference Document, KC-135 Zero Gravity Modification, Document No. D6-5353, Boeing Airplane Company, Renton, Washington, 1 April 1960.
4. Air Force Technical Orders 5F5-5-3-2, -3, -4, -12, -13, -14, Aircraft Flight Director Computer, Type GPU-4/A, Middletown Air Materiel Area, Middletown, Pennsylvania.
5. Air Force Technical Orders 5F6-3-5-3, -4, -13, -14, Gyroscope, Roll and Pitch Displacement, Type MD-1, Middletown Air Materiel Area, Middletown, Pennsylvania.
6. Air Force Technical Orders 5F6-4-3-3, -4, -13, -14, Gyroscope, Switching Rate, Type MC-1, Middletown Air Materiel Area, Middletown, Pennsylvania.
7. Air Force Technical Orders 5F8-3-11-2, -3, -4, Indicator, Attitude Director, Type ARU-2/A, Middletown Air Materiel Area, Middletown, Pennsylvania.
8. Fundamentals of Design of Piloted Aircraft Flight Control Systems, Bureau of Aeronautics, Washington, D. C. Report AE-61-4, February 1953.
9. Schock, G. J. D., and D. G. Simons, A Technique for Instrumenting Sub-gravity Flights, Air Force Missile Development Center Technical Note 58-4, Holloman Air Force Base, New Mexico, February 1958.
10. Howe, R. M., Coordinate Systems for Solving the Three-Dimensional Flight Equations, Wright Air Development Center Technical Note 55-747, Wright Patterson Air Force Base, Ohio, June 1956.
11. McRuer, D. T. and E. S. Krendel, Dynamic Response of Human Operators, Wright Air Development Center Technical Report 56-524, Wright Patterson Air Force Base, Ohio, October 1957.
12. Niehuss, O., A Preliminary Investigation of the Specific Performance Capabilities of the KC-135 Airplane for Providing Experimental Zero-Gravity Environment, Boeing Airplane Company Document D6-3885, Renton, Washington, September 1959.
13. McKinney, R., P.O.B. Montgomery, C. F. Gell and F. W. Thomas, Study of the Effects of Zero-Gravity on Cell Physiology, Chance Vought Corporation, Vought Astronautics Division and the Department of Pathology, Southwestern Medical School, Dallas, Texas, October 1961.

14. KC-135 Modification for Zero-Gravity Flight, Boeing Airplane Company, Aero Space Division, Technical Proposal D2-5358, Seattle, Washington, December 1959.
15. Modification Detail Specification for Special Test Configuration Airplane, Air Force Zero "G" Program, Boeing Airplane Company, Transport Division, Document No. D6-5169, Renton, Washington, January 4, 1960.
16. Brown, E.L., Research of Human Performance During Zero Gravity, American Society of Mechanical Engineers Report 59-AV-10, New York, 1959.
17. Bushnell, D., The History of Research in Sub Gravity and Zero G at the Air Force Missile Development Center, Holloman Air Force Base, N.M., Office of Information Service, Air Force Missile Development Center, Holloman Air Force Base, New Mexico, May 1958.
18. Gerathewohl, S.J., O.L. Ritter and H.D. Stallings, Jr., "Producing the Weightless State in Jet Aircraft," ASTRONAUTICA, ACTA, Volume 4, PP 15-24, 1958.
19. Haber, F., Study on Subgravity States, United States Air Force School of Aviation Medicine Project Number 21-34-003, Report #1, Brooks Air Force Base, Texas.
20. Haber, H. and F. Haber, "Possible Methods of Producing the Gravity-Free State for Medical Research," Journal of Aviation Medicine, Volume 21, PP 395-400, 1950.
21. Loftus, J.P. and L.R. Hammer, Weightlessness and Performance - A Review of the Literature, Aeronautical Systems Division Technical Report 61-166, Wright Patterson Air Force Base, Ohio, June 1961.
22. Shock, G.J.D., Some Observations on Orientation and Illusions When Exposed to Sub and Zero Gravity, PH.D. Thesis, University of Illinois, 1958.
23. Shock, G.J.D., Airborne Galvanic Skin Response Studies - A Preliminary Report, Air Force Missile Development Center Technical Note 59-14, Holloman Air Force Base, New Mexico, June 1959.
24. von Beckh, H.J.A., Flight Experiments About Human Reactions to Accelerations Which are Followed or Preceded by the Weightless State, Air Force Missile Development Center Technical Note 58-15, Holloman Air Force Base, New Mexico, December 1958.
25. Ward, J.E., "Requirements for Experimental Zero-Gravity Parabolas," Journal of Aviation Medicine, Volume 29: PP 428-432, 1958.
26. Flight Test Report, Initial Systems Evaluation of Zero-G Modification, Boeing Airplane Company, Document No. D6-5159, Renton, Washington, 23 June 1960.

APPENDIX A

EQUIPMENT LEADING PARTICULARS

Leading Particulars - Donner Model 4310 Linear Servo Accelerometer

Mechanical

Size	3" x 1.52" x 1.40"
Weight (max)	8 oz.
Mounting	2 holes 2.5" c-c

Electrical

Range	$\pm 1.0$ g
Output (about 14 VDC Reference)	$\pm 7.5$ VDC
Linearity (min)	0.05% full scale
Hysteresis (max)	0.02% full scale
Resolution (min)	0.0001% full scale
Natural Frequency (90° Phase Shift)	30 cps (min)
Input power	28 VDC (20 ma max)
Current Output	1 1/2 ma

Leading Particulars - Doelcam Model ZHMA-2 DC Amplifier

Mechanical

Size	6 1/2" x 5 1/4" x 8 3/8"
Weight	8 1/2 lbs.
Mounting	Shock Mounted

Electrical

Power Input	115 VAC, 400 cps (1 amp)
Input Signal (typical)	-3.8 to +5.0 MV
Output Signal	0-5 VDC
Linearity	$\pm$ 1/2% full scale
Gain Stability (max)	3%
Zero Drift (max)	$\pm$ 100 MV at input
Input Resistance (min)	1.5 K
Output Impedance (into 5000) (max)	100
Ground Configuration	Input Isolated
Frequency Response	Output - one end grounded 3db at 400 cps

APPENDIX B

TABULAR DATA

TABLE 1  
SUMMARY OF THE DATA FROM FOUR C-131B FLIGHTS

Measure	Individual Runs Summarized				
	All Runs	16 Oct	18 Oct	27 Oct	30 Oct
T <sub>05</sub>	5.13	5.6	5.7	4.3	4.7
T <sub>04</sub>	4.24	4.7	4.7	3.1	4.0
T <sub>03</sub>	2.95	3.1	3.5	2.4	2.6
T <sub>02</sub>	1.75	2.2	2.1	1.3	1.3
T <sub>01</sub>	0.65	0.3	0.9	0.6	0.6
e <sub>max</sub> (g's)	0.028	0.034	0.022	0.036	0.029
O <sub>init</sub> (g's)	0.012	--	0.011	0.012	0.013

- (a) Data from the individual flights may be found in Tables 2 through 5  
 (b) The time within a given tolerance band (T<sub>05</sub>) is in arbitrary units and is approximately one-half the time in seconds.

TABLE 2  
UNPROCESSED DATA--C-131B FLIGHT OF 16 OCT 61

Trace	Parabola	(b)					(c)	
		T <sub>05</sub>	T <sub>04</sub>	T <sub>03</sub>	T <sub>02</sub>	T <sub>01</sub>	O <sub>init</sub>	e <sub>max</sub>
6710	1	6.0	5.9	5.8	5.3	-	od <sup>(a)</sup>	0.03
6714	5	6.0	4.8	-	-	-	0.04	0.02
6715	6	7.0	6.5	3.8	1.5	-	0.02	0.01
6716	7	5.4	5.3	5.2	5.1	-	0.03	0.03
6717	8	8.2	5.5	2.0	-	-	0.02	0.07
6718	9	3.3	3.1	2.8	2.6	2.4	0.03	0.07
6720	11	4.8	4.5	3.9	2.4	-	od	0.03

- (a) od denotes that there was no initial overshoot, and that the system seemed to be overdamped.  
 (b) Units for all times within tolerance are arbitrary units, approximately one-half the time in seconds  
 (c) Units for O<sub>init</sub> and e<sub>max</sub> are "g's"

TABLE 3

## UNPROCESSED DATA--C-131B FLIGHT OF 18 OCT 1961

Trace	Parabola	T05	T04	T03	T02	T01	O <sub>init</sub>	e <sub>max</sub>
6729	1	6.5	4.0	3.8	1.5	-	.005	.032
6729	2	6.7	6.6	3.8	2.8	1.0	od	.02
6736	3	6.0	5.3	5.0	1.9	1.3	.02	.015
6736	4	6.8	4.1	1.1	-	-	od	.02
6731	5	4.5	4.1	1.8	1.7	-	.005	.02
6731	6	6.4	6.3	2.7	2.2	1.0	od	.015
6732	7	6.6	5.4	4.3	2.9	0.4	.02	.02
6732	8	3.5	1.8	-	-	-	.02	.03
6733	9	5.8	4.3	3.3	3.1	1.3	od	.03
6733	10	6.0	5.8	3.4	3.0	1.0	od	.015
6734	11	3.4	3.2	3.0	2.9	2.2	.03	.03
6734	12	7.9	6.8	6.5	1.8	0.8	.01	.01
6734	13	6.2	5.5	4.6	2.6	2.2	.02	.015
6734	14	4.2	1.6	1.1	1.0	-	.015	.03
6736	15	6.6	6.4	6.1	5.3	1.6	.01	.01
6736	16	6.1	6.0	2.7	1.2	0.8	.02	.03
6737	17	4.8	4.0	3.6	3.4	1.4	.01	.01
6737	18	4.1	3.9	1.8	-	-	.015	.03

TABLE 4

UNPROCESSED DATA--C-131B FLIGHT OF 27 OCT 1961

Trace	Parabola	T <sub>05</sub>	T <sub>04</sub>	T <sub>03</sub>	T <sub>02</sub>	T <sub>01</sub>	O <sub>init</sub>	e <sub>max</sub>
6748	2	3.6	1.4	1.1	-	-	od	.06
6749	3	1.8	1.6	1.2	-	-	od	.03
6750	4	2.9	2.8	1.8	0.6	-	.03	.03
6751	5	5.1	4.9	4.1	2.0	1.8	.02	.04
6751	6	2.9	2.1	2.1	0.7	-	.01	.03
6752	7	4.0	3.5	1.6	1.2	-	.005	.04
6753	8	7.0	5.2	4.8	4.5	2.4	.02	.027

TABLE 5

UNPROCESSED DATA--C-131B FLIGHT OF 30 OCT 1961

Trace	Parabola	T <sub>05</sub>	T <sub>04</sub>	T <sub>03</sub>	T <sub>02</sub>	T <sub>01</sub>	O <sub>init</sub>	e <sub>max</sub>
6767	1	3.4	3.3	2.4	1.9	1.7	-	.03
6769	3	4.7	4.6	3.3	2.9	1.8	.03	.015
6770	4	3.1	2.9	-	-	-	.015	.03
6771	5	5.8	2.1	1.3	1.2	0.	.01	.025
6772	6	5.1	3.3	-	-	-	.02	.03
6774	7	5.1	3.0	2.6	2.4	1.0	.02	.05
6776	9	5.9	5.7	3.9	1.4	1.3	od	.017
6777	10	5.0	4.8	4.6	1.8	-	.01	.015
6779	12	4.6	2.8	1.6	-	-	0.015	.05
6780	13	2.8	2.4	1.6	1.4	-	0.010	.025
6781	14	3.5	3.5	2.7	1.0	-	.015	.035

TABLE 6

DISTANCE FROM PARABOLA APEX OF  $T_{03}$ 

Parabola	(a) Limits of $T_{03}$
1	-0.2 to +3.6
2	-2.8 to +1.0
3	-3.2 to +1.8
4	+2.4 to +3.5
	-2.8 to -1.7
5	-3.6 to -1.8
	-1.4 to 0.0
6	-1.5 to +1.2
7	-3.2 to +1.1
8	-2.8 to +1.0
9	-1.8 to +2.1
10	-1.4 to +1.6
11	-3.5 to +3.0
12	-1.9 to +2.0
13	-3.4 to +2.7
14	-1.7 to +1.0
15	-1.7 to +1.9
16	-1.7 to +0.3

(a) Arbitrary time units from the parabola apex. "-" denotes occurrence before the apex and "+" denotes occurrence after the apex.

TABLE 7

## UNPROCESSED DATA--C-131B FLIGHT OF 3 JAN 1962

Trace	Parabola	(a)					$t_{init}$	$e_{max}$
		$T_{05}$	$T_{04}$	$T_{03}$	$T_{02}$	$T_{01}$		
7050	1	8.5	8.2	7.9	5.7	1.8	-	-
7050	2	8.6	7.7	7.2	5.8	1.5	-	-
7051	3	9.8	8.6	8.0	7.4	6.8	-	0.03
7051	4	11.3	11.1	9.9	8.7	3.8	-	-
7052	5	10.5	10.2	8.9	7.1	6.2	0.03	0.015
7052	6	10.0	9.2	7.8	6.9	3.7	-	0.015
Average		9.8	9.2	8.3	6.9	4.0		

(a) Time-within-tolerance in seconds

TABLE 8

## SUMMARY OF DATA FROM ELEVEN KC-135 FLIGHTS

Date of Flight	Number of Parabolas	T <sub>05</sub>		T <sub>04</sub>		T <sub>03</sub>		T <sub>02</sub>		T <sub>01</sub>	
16 Mar 62	11	11.03	2.5	9.98	2.3	6.77	2.1	4.07	1.8	1.43	1.1
20 Feb 62	17	10.11	3.9	8.23	4.0	6.67	3.8	4.21	2.8	1.54	1.5
24 Apr 62	15	14.17	3.3	13.40	4.0	9.30	2.6	4.56	2.7	2.63	1.3
8 Feb 62	9	13.40	2.4	12.15	3.2	9.71	3.5	6.58	3.2	2.26	1.9
12 Feb 62	17	11.74	2.5	9.40	3.5	7.68	4.1	3.96	3.0	1.61	1.5
13 Feb 62	15	8.59	3.6	7.52	3.7	4.79	3.7	2.79	2.9	0.88	1.8
13 Feb 62	18	16.10	3.6	14.85	3.4	13.10	3.4	9.75	3.1	4.70	2.5
14 Feb 62	13	15.10	4.4	13.40	4.6	12.55	4.6	8.90	4.4	4.23	2.5
16 Feb 62	20	11.56	2.7	10.00	2.7	8.35	2.3	5.25	4.1	2.21	1.4
16 Feb 62	4	10.30	1.7	9.65	2.3	8.30	2.2	4.25	0.7	1.8	1.2
19 Feb 62	14	7.73	3.4	7.14	3.1	5.28	3.0	3.75	4.4	5.58	0.8
	153										
		11.9		10.5	8.4			5.4		2.7	

TABLE 9

## TYPICAL KC-135 STOPWATCH FLOAT TIMES

DATE	1	2	3	4	5	6	7	8	9	10	11	12	13	14	15	16	17	18	19	20	T	
29 Mar	2.5	3.1	9.3	6.4	3.0	4.4	3.5	5.3	2.5	6.0	3.5	3.5	4.4	2.9	4.0						4.0	1.8
4 Apr	8.5	4.0	3.9	5.5	4.0	3.0	7.0	6.0	6.0	5.0											4.0	1.8
5 Apr	4.0	7.0	8.0	5.0	4.0	5.0	7.0	4.0	5.5												5.7	1.3
6 Apr	4.0	8.0	6.5	3.0	5.0	2.0	6.0														6.0	1.9
14 Apr	5.0	4.0	5.0	10.0	7.5	4.5															8.5	1.9
19 Apr	2.5	3.0	2.5	3.0	4.5	3.0	2.5	3.5	6.0	3.0	4.0	2.0	4.0								6.0	2.1
20 Apr	5.5	7.5	7.0	10.5	9.5																3.4	1.0
16 Jun	6.5	12.0	11.0	6.5	6.5	5.0	11.5	6.0	6.5	9.0	11.0	9.0	10.5	6.0	5.0	11.5	13.0				8.0	1.9
21 Jun	5.3	8.0	27	9.5	6.5	9.0	4.0	2.7	6.8	9.7											8.6	2.7
27 Jun	11.2	5.5	6.6	2.7	3.0	5.5	6.5	10.9	7.6	3.5	6.8	6.0									6.4	2.5
29 Jun	10.5	8.0	4.1	5.0	9.0	3.6	7.5	8.2	6.9												7.5	1.9
11 Jul	7.1	7.2	6.0	10.0	11.0	9.0	6.8	6.2	8.5	3.0											8.1	1.6
11 Jul	6.7	7.0	5.5	5.4		6.0	7.5	7.0													6.0	0.7
11 Jul	11.0	11.0	10.5	5.5	6.0	7.5	7.0														8.0	2.2
19 Jul	21.5	11.3	13.5	6.0	2.3	4.0	1.5	5.1	7.3	5.8	4.8	7.0	6.4	7.8							7.0	5.0
6 Feb	6.0	11.0	10.0	4.0	3.0	4.0	4.0	5.0													6.0	2.9
8 Feb	2.0	4.4	4.0	8.0	4.0	3.5	3.5	5.5	3.0												4.0	1.6
13 Feb	3.5	3.0	7.5	7.0	10.0	4.0	10.0	6.5	3.0	4.0	14.5	13.0	13.0	14.5							9.0	3.4
13 Feb	3.2	2.0	5.6	3.6	2.6	0.8	4.2	4.3	3.2	3.1	0.1	9.6	6.0	2.4	3.0	4.3	1.2	0.9			3.0	2.2
14 Feb	5.3	3.9	6.1	7.7	6.9	3.6	1.3	2.5	2.5	2.6	1.3	5.2	4.3	4.2	4.3	2.8	4.8	3.3	1.5	5.0	4.0	1.7
15 Feb	6.0	11.0	7.3	7.3	12.0	3.3	14.3	10.5	8.1	13.9	12.5	8.2	11.3	5.5	8.5						9.0	3.1
15 Feb	12.0	14.0	14.0	18.0																	14.0	2.2
16 Feb	3.0	6.0	4.5	5.0	6.5	5.5	5.0	4.0	19.5	15.0											4.0	1.1
7 Feb	2.0	11.0	7.0	3.5	5.0	11.5	11.0	16.0	8.0	5.0											7.0	7.0
12 Feb	10.0	2.0	3.0	1.0	5.0	11.5	11.0	16.0	8.0	5.0											7.0	7.0
20 Feb	2.0	4.0	1.0	6.0	4.0	2.0	7.0	4.0	15.0	4.0	1.0	3.0	3.0	2.0	2.0	2.0	2.0	4.0			4.0	4.0
16 Feb	7.0	5.9	9.0	4.2	9.1	15.2	9.6	12.0	10.0	5.0	11.0	9.5	6.0								8.0	8.0

APPENDIX C

DEVELOPMENT OF SIMULATION EQUATIONS

## DEVELOPMENT OF SIMULATION EQUATIONS

### Three Degree-of-Freedom Equations of Motion

The longitudinal equations of motion of the aircraft relative to the body axes of the aircraft are:

$$\sum X_i = m(\dot{U} + WQ) \quad (1)$$

$$\sum Z_i = m(\dot{W} - UQ) \quad (2)$$

$$\sum M_i = I_{yy}\dot{Q} \quad (3)$$

The quantities  $U$ ,  $W$  and  $Q$  are the linear velocities of the aircraft in the  $X$  and  $Z$  directions, and the angular (inertial) body rate about the  $Y$  axis, respectively. Sideslip, or linear velocity along the aircraft  $Y$  axis is assumed to be zero, and the roll and yaw body rates are assumed to be small enough to be neglected. The three rates  $U$ ,  $W$  and  $Q$  are taken in this formulation to be the total velocities in or about their respective axes, and are not the perturbed quantities.

These quantities may be found in Figure 33 with definition of their positive directions.

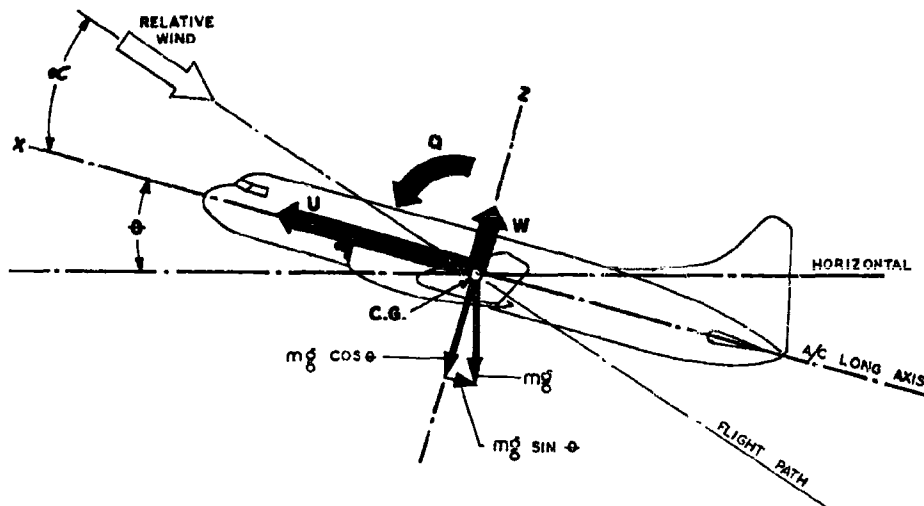


Figure 33. Definition of Axes and Angles

### Gravity Force

The force due to gravity may be resolved from the set of Earth axes to the aircraft body axes quite simply by reference to Figure 33. This rotation yields the resolved forces:

$$X_g = -mg \sin \theta \quad (4)$$

$$Z_g = -mg \cos \theta \quad (5)$$

### Thrust Force

The thrust is assumed to act through the Center of Gravity of the aircraft and to be coincident with the X-axis. We therefore get as the components of thrust:

$$X_T = T_o + \Delta T = T_o + T_{\delta} \frac{\delta}{\text{rpm}} \quad (6)$$

$$Z_T = M_T = 0 \quad (7)$$

The thrust component  $T_o$  is the steady state thrust for straight and level flight with no loss of airspeed at the trim condition determined at the beginning of the simulation run. The other component is the incremental thrust change which represents the co-pilot movement of the throttles. Change of thrust due to ram effect is taken into account in the thrust approximation.

### Aerodynamic Forces

The aerodynamic forces are all developed in the stability axis system and then are resolved into the body axis system for summation with the thrust and gravity forces in the equations of motion.

The total aircraft velocity  $V_p$  is the vector sum of the body velocities U, V, and W, and, if V is zero, then the angle between  $V_p$  and U is defined as  $\alpha$ , the angle of attack.

$$V_p = \frac{U}{\cos \alpha} \quad (8)$$

$$\tan \alpha = \frac{W}{U} \quad (9)$$

The force  $X_g$  along the longitudinal stability axis may be broken down into forces dependent upon longitudinal velocity U, angle of attack  $\alpha$ , and elevator deflection  $\delta_e$ :

$$x_s \triangleq x_{u,\alpha} + x_{\delta_e} \quad (10)$$

$$x_{u,\alpha} = \frac{-fSU^2}{2} C_D, \text{ where } C_D \triangleq C_{D_0} + 0.04C_L^2 \quad (11)$$

$$x_{\delta_e} = 0 \quad (12)$$

The contributions to  $Z_s$  are due to changes in  $U$ ,  $\alpha$ ,  $\dot{\alpha}$ ,  $Q$ , and  $\delta_e$ , and may be formulated as:

$$Z_s = Z_{u,\alpha} + Z_{\dot{\alpha}} + Z_Q + Z_{\delta_e} \quad (13)$$

$$Z_{u,\alpha} = \frac{-fU^2s}{2} C_L, \text{ where } C_L = C_{L\alpha} \alpha \quad (14)$$

$$Z_{\dot{\alpha}} = \frac{-fS\bar{c}U}{4} C_{L\dot{\alpha}} \dot{\alpha} \quad (15)$$

$$Z_Q = \frac{-fS\bar{c}U}{4} C_{LQ} Q \quad (16)$$

$$Z_{\delta_e} = \frac{-fU^2s}{2} C_{L\delta_e} \delta_e \quad (17)$$

The contributions to  $M_s$  are due to changes in  $\alpha$ ,  $\dot{\alpha}$ ,  $Q$  and  $\delta_e$ , and may be formulated as:

$$M_s = M_{\alpha} + M_{\dot{\alpha}} + M_Q + M_{\delta_e} \quad (18)$$

$$M_{\alpha} = \frac{fU^2s\bar{c}}{2} C_{m\alpha} \alpha \quad (19)$$

$$M_Q = \frac{fUS\bar{c}^{-2}}{4} C_{mQ} Q \quad (20)$$

$$M_{\alpha} = \frac{\rho S \bar{c}^2 U}{4} C_{m_{\alpha}} \alpha \quad (21)$$

$$M_{\delta_e} = \frac{\rho S U^2 \bar{c}}{2} C_{m_{\delta_e}} \delta_e \quad (22)$$

Resolution of Aerodynamic Forces on to Body Axes:

Rotation of the aerodynamic stability axis into the body axis system is a rotation through angle  $\alpha$ , and gives the aerodynamic forces X, Z and M in terms of the stability axis quantities  $X_S$ ,  $Z_S$ , and  $M_S$ .

$$X = X_S \cos \alpha - Z_S \sin \alpha \quad (23)$$

$$Z = Z_S \cos \alpha + X_S \sin \alpha \quad (24)$$

$$M = M_S \quad (25)$$

Resolution of Body Rate onto Euler Rate

$$-\dot{\theta} = Q \quad (26)$$

Resolution of Euler Angles and Body Velocities into Earth Coordinates

The rotation of the body axes through angle  $\theta$  resolves the body axis quantities into earth coordinates  $\dot{s}_x$ ,  $\dot{s}_y$  and  $\dot{s}_z$ .

$$\dot{s}_x = U \cos \theta - W \sin \theta \quad (27)$$

$$\dot{s}_z = W \cos \theta + U \sin \theta \quad (28)$$

This completes the equations of motion for the longitudinal dynamics of the C-131B.

### Pilot Transfer Function

It has been shown in studies of the dynamics of a human in a control system that the operator, or pilot, has the ability to adapt himself to the complexity of the task (Reference 11). Therefore, there is no one human transfer function, and the best that can be done is to choose a task which is roughly similar to the one we have, and for which a human model exists, and use this transfer function as the first attempt in the closed loop. The transfer function chosen was one derived in studies of a pilot in a "tail-chasing" task, with the system dynamics including a double integration, quadratic lag, and two lead terms. (This work was done by the Franklin Institute and is described in Reference 11). The human transfer function for the pilot was of the form:

$$\frac{K_p e^{-\tau s} (\tau_L s + 1)}{(\tau_I s + 1) (\tau_N s + 1)} \quad \text{where } K_p$$

is the pilot's gain,  $\tau_L$  and  $\tau_I$  are the pilot's lead-lag compensation,  $\tau_N$  is the pilot's neuromuscular lag, and  $\tau$  is the pilot's reaction time constant.

### Reaction Time Simulation

The pilot's reaction time term,  $e^{-\tau s}$ , will be approximated by two second order ratios of polynomials. The approximating equations take the form:

$$e^{-\tau s} \approx \frac{1 - 2\zeta_1 s + \tau^2 s^2}{1 + 2\zeta_2 s + \tau^2 s^2} \frac{1 - 2\zeta_2 s + \tau^2 s^2}{1 + 2\zeta_1 s + \tau^2 s^2}$$

### Trim Integration

A display error integration function is put into the pilot model to account for aircraft trim changes. Elevator deflection for aircraft pitch trim during the parabola changes drastically. In order to maintain a constant pitch trim condition with a corresponding zero display error, it is necessary to introduce an integration of the display error into the commanded elevator position, and this is mechanized as shown in Figure 34.

### Arbitrary Function Generator (G-Programmer)

The g-programmer shall generate a g-profile which may be described as follows (Figure 35):

Origin to Point (1): constant 0.75 g until U = 250 knots

Point (1) to Point (2): constant 2-1/2 g until  $\theta = 35^\circ$

Point (2) to Point (3): constant 0 g until  $\theta = -35^\circ$

Point (3) to Point (4): constant 2-1/2 g until  $\theta = 0^\circ$

Point (4) to End: constant 1.0 g

All changes in g-level occur through a second order time lag with time constant and damping to be optimized.

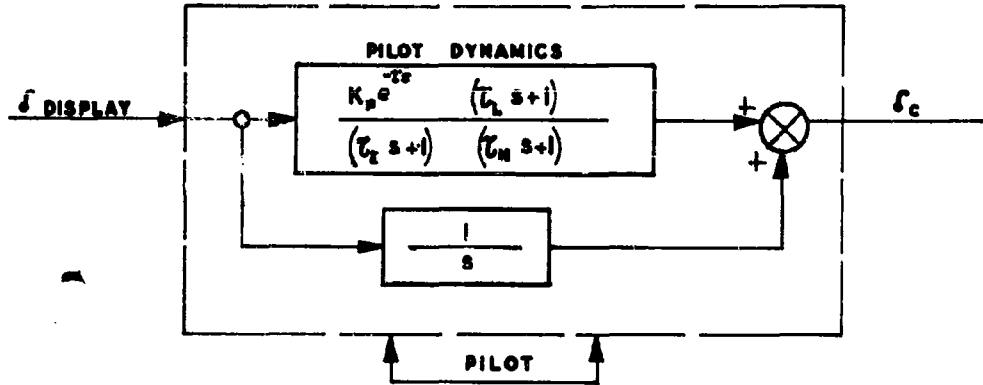


Figure 34. Pilot Model

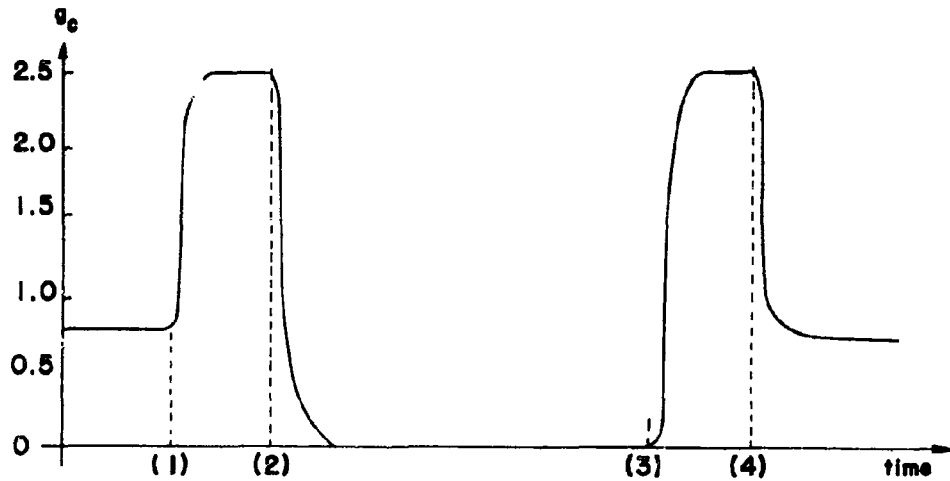


Figure 35. Arbitrary Function Generator (G-Programmer)

### Display and Display Compensation

The Display and Display Compensation shall consist of a static gain and a lead-lag. For the initial phase of the simulation the lead shall be omitted, and the static display gain set at 0.8 inches per 0.2 g. Value of the lag time constant shall be one-half second.

### Co-Pilot Dynamics

The Co-pilot shall be represented by a simple gain  $K_{cp}$ .

### Throttle Display

The Throttle Display shall likewise be represented by a simple gain  $K_{td}$ .

### Throttle Control Dynamics

The Throttle Control Dynamics shall be simulated by a gain  $K_{RPM}$  and a single order lag with time constant of one second.

### RECORDED QUANTITIES

The following quantities shall be recorded:

Airspeed	$U$	Knots (0 to 300)
Normal Acceleration	$\frac{\dot{W} + 1\dot{Q} - UQ}{g} \cos \theta$	g's (-1 to +3)
Elevator Deflection	$\delta_e$	deg. (-20 to +20)
Altitude	$\int \dot{z}$	feet (0 to 20K)
Pitch Angle	$\theta$	deg. (-50 to +50)
G-Programmer Output	$g_c$	g's (-1 to +3)
Display Error	$\delta_d$	inches (+ 3)
Throttle Command	$\delta_{rpm}$	$\Delta$ rpm (+1000)
Longitudinal Accelerometer	$A = \frac{\dot{U} + WQ}{g} + \sin \theta$	g's (+1 to -1)

Aerospace Medical Division,  
6570th Aerospace Medical Research  
Laboratories, Wright-Patterson AFB, Ohio  
Rpt. No. AMRL-TDR-63-11. DISPLAY SYSTEMS  
FOR SUB- AND ZERO- GRAVITY FLIGHT  
Final Report Jan 63, x + 54 p. incl. illus.,  
tables, 26 refs. Unclassified report

A study was performed of the controls and  
pilot displays used to fly a C-131B and KC-135  
aircraft in a Keplerian trajectory to create  
zero-gravity conditions. Evaluation criteria  
for this maneuver were proposed and applied  
to two basic instrumentation systems which  
were developed. An analog simulation was  
formulated and these results will be used to  
further improve the systems.

( over )

Recommendations are made for  
improved instrumentation which  
should enable consistent flights of 10 seconds  
at zero-gravity plus or minus 0.005g.

UNCLASSIFIED

1. Keplerian Trajectory
2. Weightlessness
3. Control and Pilot Displays
4. Analog Simulation
5. Instrument Panels

I. AFSC Project 7184,  
Task 718405

II. Behavioral Sciences  
Laboratory

III. Contract AF 33(657)-  
7199

IV. Lear Siegler, Inc.  
Grand Rapids, Mich.

V. R. Weiss

UNCLASSIFIED

UNCLASSIFIED

VI. In ASTIA collection  
VII. Aval fr OTS: \$1.75

UNCLASSIFIED

Aerospace Medical Division,  
6570th Aerospace Medical Research  
Laboratories, Wright-Patterson AFB, Ohio  
Rpt. No. AMRL-TDR-63-11. DISPLAY SYSTEMS  
FOR SUB- AND ZERO- GRAVITY FLIGHT  
Final Report Jan 63, x + 54 pp. incl. illus.,  
tables, 26 refs. Unclassified report

A study was performed of the controls and  
pilot displays used to fly a C-131B and KC-135  
aircraft in a Keplerian trajectory to create  
zero-gravity conditions. Evaluation criteria  
for this maneuver were proposed and applied  
to two basic instrumentation systems which  
were developed. An analog simulation was  
formulated and these results will be used to  
further improve the systems.

( over )

Recommendations are made for  
improved instrumentation which  
should enable consistent flights of 10 seconds  
at zero-gravity plus or minus 0.005g.

UNCLASSIFIED

1. Keplerian Trajectory
2. Weightlessness
3. Control and Pilot Displays
4. Analog Simulation
5. Instrument Panels

I. AFSC Project 7184,  
Task 718405

II. Behavioral Sciences  
Laboratory

III. Contract AF 33(657)-  
7199

IV. Lear Siegler, Inc.  
Grand Rapids, Mich.

V. R. Weiss

UNCLASSIFIED

UNCLASSIFIED

VI. In ASTIA collection  
VII. Aval fr OTS: \$1.75

UNCLASSIFIED